

EFFECTS OF METHYLMERCURY AND THEAFLAVIN DIGALLATE ON ADIPOKINES IN
MATURE 3T3-L1 ADIPOCYTES

By

Shubhangi Chauhan, B.Tech

A Thesis Submitted in Partial Fulfillment of the Requirements

for the Degree of

Master of Science

in

Biochemistry and Neuroscience

University of Alaska Fairbanks

May 2019

APPROVED:

Dr. Lawrence Duffy, Committee Chair
Dr. Kelly Drew, Committee Member
Dr. Kriya Dunlap, Committee Member
Dr. Thomas Green, Chair
Department of Chemistry & Biochemistry
Dr. Leah Berman, Interim Dean
College of Natural Science & Mathematics
Dr. Michael Castellini, Dean
Graduate School

Abstract

Diabetes is a contributor to morbidity across the globe and is often associated with obesity, metabolic syndrome and other inflammatory diseases associated with aging. In addition to genetic and lifestyle factors, environmental factors such as metals and persistent organic pollutants may increase the severity or lower the threshold of these conditions. In cell culture, methylmercury is toxic to adipocytes and may impact the adipokine secretions. In this study, I determined the effects of different concentrations of theaflavin digallate on methylmercury exposed 3T3-L1 adipocytes in cell culture. Secretions of resistin, adiponectin and lipid peroxidation product, 4-HNE were monitored using ELISA assays from Day 18 to 28. Cell morphology was assessed over the period of ten days and on day 28 was observed using Lipid (Oil Red O) staining.

Results showed that exposure to methylmercury increased the levels of resistin and adiponectin as well as 4-HNE when compared to the control cells. Methylmercury treated cells resulted in smaller and highly clumped lipid droplets. These results suggest that methylmercury induces reactive oxygen species leading to development of an inflammatory response. Theaflavin digallate reduced the impact of methylmercury by restoring the morphology and secretion patterns of adiponectin, resistin and 4-HNE. With this enhanced signaling model other anti-inflammatory agents could be tested at this biochemical level eventually leading to studies in animal models.

Table of Contents

Title Page.....	i
Abstract	ii
Table of Contents	iii
List of Figures	vii
List of Tables.....	xi
List of Abbreviations.....	xii
Acknowledgements.....	xiii
Chapter 1 Introduction.....	1
1.1 Methylmercury and its role in generating oxidative stress.....	1
1.2 Adipokines and Anti-Inflammatory agents.....	3
1.3 Adipose tissue.....	5
1.4 3T3-L1 cell line.....	6
1.5 Adipokines.....	7
1.5.1 Adiponectin.....	8
1.5.2 Resistin.....	9
1.6 Cell model approach.....	10
1.7 Research Hypotheses.....	11

Chapter 2 Materials and Methods.....	12
2.1 Cell Culture.....	12
2.2 Treatment with toxin and antioxidant.....	16
2.3 Safety.....	17
2.4 Morphology: Lipid (Oil Red O) Staining.....	18
2.5 Enzyme Linked Immunosorbent Assay (ELISA).....	19
2.5.1 Sandwich ELISA: Adiponectin	21
2.5.2: Sandwich ELISA: Resistin.....	22
2.5.3: Competitive ELISA: Mouse 4-Hydroxynonenal (4-HNE).....	24
2.6 Statistical analysis.....	25
Chapter 3 Results.....	27
3.1 Morphology.....	27
3.1.1. Morphological changes in 3T3-L1 cell line to form mature 3T3-L1 adipocytes.....	27
3.1.2 Morphological changes in 3T3-L1 adipocytes on Day 20 upon exposure to MeHg and TF-3.....	29
3.1.3 Morphological changes in 3T3-L1 adipocytes on Day 22 upon exposure to MeHg and TF-3.....	32
3.1.4 Morphological changes in 3T3-L1 adipocytes on Day 24 upon exposure to MeHg and TF-3.....	35
3.1.5 Morphological changes in 3T3-L1 adipocytes on Day 26 upon exposure to MeHg and TF-3.....	37
3.1.6 Morphological changes in 3T3-L1 adipocytes on Day 28 upon exposure to MeHg and TF-3 using Oil Red O.....	40

3.2 Effects of MeHg and TF-3 on the secretion patterns of adiponectin.....	43
3.2.1 Basal levels of adiponectin secreted from control population of 3T3-L1 cells.....	43
3.2.2 Effect of MeHg exposure on adiponectin secretion from 3T3-L1 cells (Day 18 - Day 28).....	44
3.2.3 Effect of MeHg+3.14 μ M TF-3 exposure on adiponectin secretion from 3T3-L1 cells (Day 18 - Day 28).....	45
3.2.4 Effect of MeHg+6.25 μ M TF-3 exposure on adiponectin secretion from 3T3-L1 cells (Day 18 - Day 28).....	46
3.2.5 Effect of MeHg+12.5 μ M TF-3 exposure on adiponectin secretion from 3T3-L1 cells (Day 18 - Day 28).....	47
3.2.6 Effect of MeHg+25 μ M TF-3 exposure on adiponectin secretion from 3T3-L1 cells (Day 18-Day 28)	48
3.2.7 Effect of MeHg+50 μ M TF-3 exposure on adiponectin secretion from 3T3-L1 cells (Day 18-Day 28)	49
3.2.8 Effect of MeHg+100 μ M TF-3 exposure on adiponectin secretion from 3T3-L1 cells (Day 18-Day 28).....	50
3.2.9 Overall analysis of adiponectin concentrations from population 1 to population 8.....	51
3.3 Effects of MeHg and TF-3 on the secretion patterns of resistin.....	53
3.3.1 Basal levels of resistin secreted from control population of 3T3-L1 cells....	53
3.3.2 Effect of MeHg exposure on resistin secretion from 3T3-L1 cells (Day 18-28).....	54
3.3.3 Effect of MeHg+3.14 μ M TF-3 exposure on resistin secretion from 3T3-L1 cells (Day 18-Day 28).....	55

3.3.4 Effect of MeHg+6.25 μ M TF-3 exposure on resistin secretion from 3T3-L1 cells (Day 18-Day 28).....	56
3.3.5 Effect of MeHg+12.5 μ M TF-3 exposure on resistin secretion from 3T3-L1 cells (Day 18-Day 28).....	57
3.3.6 Effect of MeHg+25 μ M TF-3 exposure on resistin secretion from 3T3-L1 cells (Day 18-Day 28).....	58
3.3.7 Effect of MeHg+50 μ M and MeHg+100 μ M TF-3 exposure on resistin secretion from 3T3-L1 cells (Day 18 - Day 28).....	59
3.3.8 Overall analysis of resistin concentrations from population 1 to population 8.....	61
3.4 Effects of MeHg and TF-3 on 4-HNE secreted from 3T3-L1 adipocytes.....	63
3.4.1 Basal 4-HNE levels secreted from 3T3-L1 adipocytes.....	63
3.4.2 Effects of MeHg and MeHg+TF-3 on the secretion of 4-HNE level.....	64
Chapter 4 Discussion.....	69
4.1 Morphology changes in 3T3-L1 adipocytes.....	70
4.2 Adiponectin secretion from MeHg exposed 3T3-L1 adipocytes and counter effects of TF-3 on MeHg exposed cells.....	71
4.3 Resistin secretion from MeHg exposed 3T3-L1 adipocytes and counter effects of TF-3 on MeHg exposed cells.....	72
4.4 4-HNE secretion from MeHg exposed 3T3-L1 adipocytes and counter effects of TF-3 on MeHg exposed cells.....	73
4.5 Future directions.....	73
References.....	75

List of Figures

Figure 1.1: Chemical structure of the black tea derived polyphenol, theaflavin digallate.....	4
Figure 1.2: Essential biological roles exhibited by the White Adipose Tissue (WAT).....	6
Figure 1.3: In vitro differentiation process of 3T3-L1 cell line to form mature adipocytes.....	7
Figure 1.4: Adipokines secretion from adipocytes under normal and abnormal metabolic conditions.....	8
Figure 2.1: Timeline of exposure study.....	13
Figure 2.2: Schematic of basic sandwich ELISA technique.....	19
Figure 2.3: Adiponectin Standard Curve.....	22
Figure 2.4: Resistin Standard Curve.....	23
Figure 2.5: 4-HNE Standard Curve.....	25
Figure 3.1a: 3T3-L1 pre-adipocytes (Day 2).....	27
Figure 3.1b: 3T3-L1 differentiating adipocytes (Day 18).....	28
Figure 3.1c: Mature 3T3-L1 adipocytes (Day 28).....	29
Figure 3.1d: Morphology changes caused due to different treatments to mature adipocytes on Day 20.....	31
Figure 3.1e: Morphology changes caused due to different treatments to mature adipocytes on Day 22.....	34

Figure 3.1f: Morphology changes caused due to different treatments to mature adipocytes on Day 24.....	36
Figure 3.1g: Morphology changes caused due to different treatments to mature adipocytes on Day 26.....	39
Figure 3.1h: Morphology changes caused due to different treatments to mature adipocytes on Day 28 using lipid staining.....	41
Figure 3.2a: Basal adiponectin levels secreted from 3T3-L1 cells (Day 0 to Day 28).....	44
Figure 3.2b: Adiponectin secretion from control cells (population 1) and MeHg exposed cells (population 2) from day 20- day 28.....	45
Figure 3.2c: Adiponectin secretion from control cells (population 1) and MeHg + 3.14 μ M TF-3 exposed cells (population 3) from day 18- day 28.....	46
Figure 3.2d: Adiponectin secretion from control cells (population 1) and MeHg + 6.25 μ M TF-3 exposed cells (population 4) from day 18- day 28.....	47
Figure 3.2e: Adiponectin secretion from control cells (population 1) and MeHg + 12.5 μ M TF-3 exposed cells (population 5) from day 18- day 28.....	48
Figure 3.2f: Adiponectin secretion from control cells (population 1) and MeHg + 25 μ M TF-3 exposed cells (population 6) from day 18 - day 28.....	49
Figure 3.2g: Adiponectin secretion from control cells (population 1) and MeHg + 50 μ M TF-3 exposed cells (population 7) from day 18- day 28.....	50
Figure 3.2h: Adiponectin secretion from control cells (population 1) and MeHg + 100 μ M TF-3 exposed cells (population 8) from day 18 - day 28.....	51

Figure 3.2i: Adiponectin secretion in all eight populations from day 18 - day 28.....	52
Figure 3.3a: Basal resistin levels secreted from 3T3-L1 cells (Day 0 to Day 28).....	54
Figure 3.3b: Resistin secretion from control cells (population 1) and MeHg exposed cells (population 2) from day 18 - day 28.....	55
Figure 3.3c: Resistin secretion from control cells (population 1) and MeHg + 3.14 μ M TF-3 exposed cells (population 3) from day 18 - day 28.....	56
Figure 3.3d: Resistin secretion from control cells (population 1) and MeHg + 6.25 μ M TF-3 exposed cells (population 4) from day 18 - day 28.....	57
Figure 3.3e: Resistin secretion from control cells (population 1) and MeHg + 12.5 μ M TF-3 exposed cells (population 5) from day 18 - day 28.....	58
Figure 3.3f: Resistin secretion from control cells (population 1) and MeHg + 25 μ M TF-3 exposed cells (population 6) from day 18 - day 28	59
Figure 3.3g: Resistin secretion from control cells (population 1) and MeHg + 50 μ M TF-3 exposed cells (population 7) from day 18 - day 28.....	60
Figure 3.3h: Resistin secretion from control cells (population 1) and MeHg + 100 μ M TF-3 exposed cells (population 8) from day 18 - day 28.....	60
Figure 3.3i: Resistin secretion in all eight populations from day 18 - day 28.....	62
Figure 3.4a: Basal 4-HNE levels secreted from 3T3-L1 cells (Day 0 to Day 28).....	63
Figure 3.4b: 4-HNE secretion from control cells (population 1) and MeHg exposed cells (population 2) from day 18 - day 28.....	64

Figure 3.4c: 4-HNE secretion from control cells (population 1) and MeHg + 3.14 μ M TF-3 exposed cells (population 3) from day 18 - day 28.....	65
Figure 3.4d: 4-HNE secretion from control cells (population 1) and MeHg + 6.25 μ M TF-3 exposed cells (population 4) from day 18 - day 28.....	66
Figure 3.4e: 4-HNE secretion from control cells (population 1) and MeHg + 12.5 μ M TF-3 exposed cells (population 5) from day 18 - day 28.....	66
Figure 3.4f: 4-HNE secretion from control cells (population 1) and MeHg + 25 μ M TF-3 exposed cells (population 6) from day 18 - day 28.....	67
Figure 3.3g: 4-HNE secretion from control cells (population 1) and MeHg + 50 μ M TF-3 exposed cells (population 7) from day 18 - day 28.....	67
Figure 3.4h: 4-HNE secretion from control cells (population 1) and MeHg + 100 μ M TF-3 exposed cells (population 8) from day 18 - day 28.....	68

List of Tables

Table 2.1: List showing study groups of different populations.....	13
Table 2.2: Cell Culture Protocol.....	14
Table 2.3: Chemical components for 3T3-L1 cell culture media.....	15
Table 2.4: Liquid media composition of culture wells plate.....	17

List of Abbreviations

ATCC	American Type Culture Collection
DMEM	Dulbecco's Modified Eagle Medium
ELISA	Enzyme-linked immunosorbent assay
FBS	Fetal bovine serum
IBMX	Methylisobutylxanthine
MeHg	Methylmercury
MetS	Metabolic Syndrome
ng/mL	Nanograms per milliliter
pg/mL	Picograms per milliliter
ppm	Parts per million
ROS	Reactive Oxygen Species
rpm	Revolutions per minute
RT	Room temperature
TF-3	Theaflavin-3,3'-digallate
VEGF	Vascular endothelial growth factor
WAT	White Adipose Tissue

Acknowledgements

I wish to acknowledge support from the University of Alaska, Fairbanks, Department of Chemistry and Biochemistry, Alzheimer Disease Resource Agency of Alaska, and Institute of Arctic Biology Graduate Summer Research Award.

In this thesis, Chapter 1 was modified from Chauhan, S. D. (2018). Methyl Mercury, Adipokines, 3T3-L1 Cells and Diabetes. *Advances in Clinical Toxicology*, 3 (4), 1-6. Chapters 2 through 4 will be prepared for submission in a scientific journal.

I want to express sincere gratitude to my advisor, Dr. Lawrence Duffy, for his incessant support in my graduate program and my thesis. I also want to thank my committee members Kelly Drew and Kriya Dunlap for their guidance and feedback throughout the process. I would be remiss if I do not acknowledge my colleagues, Aline Collin, Theresa Vertigan and Ranjan Dissanayake, for their help in my research.

My graduate program would not have been possible without the encouragement and blessings from my family.

Chapter 1: Introduction

1.1 Methylmercury and its role in generating oxidative stress

Methylmercury (MeHg) is historically known to pose a threat to the ecosystem. MeHg, a potent neurotoxin, bioaccumulates and biomagnifies through the ecosystem and eventually up to human beings (United States Environmental Protection Agency, 2015). Eighty - Ninety percent of organic mercury present in humans is from fish and shellfish intake (Hong et al., 2012) MeHg crosses the human placenta and can impair the developing fetus (Mahaffey, 1999). Arctic communities residing in rural Alaska rely highly on fish as a staple food (Lemire et al., 2015). Recent epidemiological studies suggest a correlation between MeHg exposure and eventual development of type 2 diabetes and hypertension (He et al., 2013; Wu et al., 2018).

Many studies in the neurotoxicity of MeHg have been conducted on the underlying mechanism (Weiss, 2007; Kanda et al., 2014; Kerper et al., 1992; Kumagai et al., 2013). The potential impact of MeHg exposure on other organ or cell types has not been as extensively studied. In 2003, Barnes et al. reported the effect of inorganic mercuric chloride on the process of adipogenesis which showed that mercury exposure can inhibit the differentiation process of pre-adipocytes (Barnes et al., 2003). Later, it was also reported that the addition of mercuric chloride to the differentiated 3T3-L1 cells increased glucose transport into the adipocytes (Barnes et al., 2005).

To the best of our knowledge, only one study exists which has examined the effect of MeHg on the adipocytes, the specialized cells of the adipose tissue. In studying the cytokine Vascular Endothelium Growth Factor (VEGF) expression by 3T3-L1 cells, Vertigan et al. observed that an exposure of 100 ng/ml (0.4 μ M) of MeHg is cytotoxic to adipocytes (Vertigan et al., 2017). Additionally, they found that 0.4 μ M MeHg exposure elevates the VEGF secretion during later stages of differentiation.

However, the effect of MeHg on the mature 3T3-L1 adipocytes and on secreted adipokines such as adiponectin and resistin, associated with the development of disease has not been well studied. Moreover, no study exists on mitigating the negative effects of MeHg exposure associated with the diet. Cell culture studies on 3T3-L1 cell line provide an experimental model for studying the effects of MeHg exposure and other contaminants on adipose tissue (Brody et al., 2009; Fasshauer et al., 2003). MeHg has a high affinity for sulfhydryl protein groups leading to S-mercuration. S-mercuration of cellular proteins is assumed to be involved in the mechanism underlying MeHg toxicity (Kanda et al., 2014). In cells, MeHg undergoes reactions that increase the release of free radicals such as reactive oxygen species (ROS) (Hong et al., 2012). ROS causes oxidative stress and lipid peroxidation which has been suggested as a cause for the insulin resistance associated with obesity and type 2 diabetes (Heilbronn & Campbell, 2008; Borza et al., 2013).

4-hydroxynonenal (4-HNE), an α , β -unsaturated hydroxyalkenal, is a common product of lipid peroxidation and is used as a biomarker for oxidative stress in cells (Zhong & Yin, 2015). MeHg exposure may increase ROS levels which would increase lipid peroxidation resulting in the greater production of 4-HNE (Borza et al., 2013) and an inflammation of the tissue. 4-HNE is also found to have role in obesity, the metabolic syndrome, and associated vascular and neurodegenerative disorder (Mattson, 2009). Since low levels of MeHg are present in many foods, and is fat soluble, it is reasonable to hypothesize its relationship to adipokines in the exacerbation of inflammation (Apprahamian & Sam, 2011). Additionally, Timar et al. suggested that adipose tissue secreted cytokines are involved in initiation and stimulation of pro-inflammatory status, which contributes to insulin resistance (Timar et al., 2014).

A cell culture model that can investigate MeHg mixtures with low levels of other contaminants would be useful (Magueresse-Battistoni et al., 2018). The significance of a model focusing on the cell culture hierarchical level is threefold. First, there is a greater precision in measurement of the interaction of the adipokines in controlled experiments. Secondly, there is

an increasing literature linking oxidative stress to inflammation, diabetes and metabolic syndrome (Met S). Thirdly, the cell culture system is easily adaptable to using multiple stressors such as mixtures of metals and endocrine disruptors. Such a design and the measure of the changes in various adipokines levels would give a more realistic picture of the impact of environmental exposure. The response of the adipokines in this model would provide the basis for new strategies in disease management.

A significant public health issue is how exposure to metals aggravates a disease or syndrome. Understanding the impact of various metals, as well as mixtures, on the etiology of hypertension, diabetes and arthritis is needed to clarify the underlying mechanisms such as the role of the balance of antioxidants and oxidants as well as pre- and anti- inflammatory cytokines and adipokines (Chen et al., 2006; Magueresse-Battistoni et al., 2018).

1.2 Adipokines and Anti-Inflammatory Agents

Adipokines such as adiponectin and resistin are proteins which are secreted from the adipocytes and are potential markers for hypertension and metabolic syndrome (Brody et al., 2009; Zhang et al., 2015a). Anti-inflammatory agents may mitigate the effect of MeHg by reducing the amount of ROS formed. A natural compound derived from black tea possesses anti- inflammatory properties and it might be a potential therapeutic candidate for reducing inflammation (Wu et al., 2017). Theaflavin-3,3'- digallate (TF- 3) one of the species of theaflavins, possess several active properties, one of which is the ability to fight ovarian cancer (Miao et al., 2013; Gao et al., 2015). Natural products like organic tea compounds might protect individuals exposed to the normal concentration of MeHg found in Alaskan subsistence foods (Hamade, 2014).

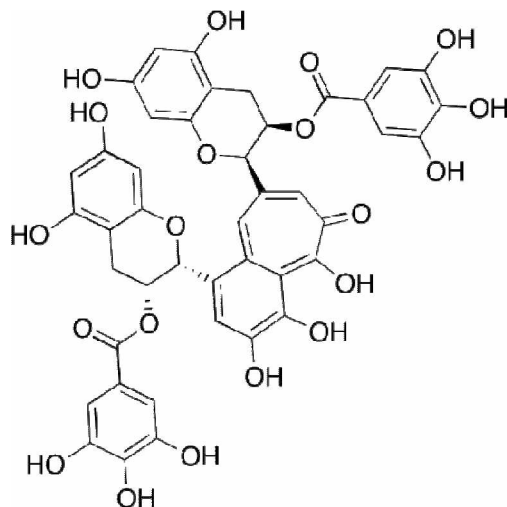


Figure 1.1: Chemical structure of the black tea derived polyphenol, theaflavin digallate

Obesity has also been linked with type 2 diabetes (Kahn et al., 2006; Murdolo & Smith, 2006; Bays et al., 2008). Preliminary investigations regarding the effects of MeHg exposure on adipocytes will enhance the existing knowledge in this area of research. A central question addressed here is, “If MeHg increases basal ROS levels, would it interfere with adiponectin and resistin secretion patterns, thereby alternating insulin sensitivity and regulation of glucose transport?” Natural compounds such as theaflavin-3,3'-digallate (TF-3) should be tested to observe their effect on MeHg interference on the secretion of adipokines.

Alaskans eat, on average, more fish than the average American, since many living in rural Alaska have to rely on fish for subsistence (World Health Organization, 1990; Nobmann et al., 1992; Ballew et al., 2004; Krabbenhoft & Sunderland, 2013; Erickson & Lin, 2015). Obesity rates are rising among Alaska Native populations and the amount of mercury found in the environment in Arctic regions has also been rising (Makhoul et al., 2010). Barnes et al., and Vertigan et al., have studied the effects on the 3T3 –L1 cells (Barnes et al., 2003, 2005; Vertigan et al., 2017). It has been reported that MeHg exposure of 100 ng/ml is cytotoxic to the

3T3 L1 cells and also increases VEGF secretion during later stages of differentiation (Vertigan et al., 2017). Here I study the effect of MeHg on ROS levels and the effect of TF on adipokines release from 3T3-L1 cells.

Epidemiological studies suggest a correlation between the mercury exposure and eventual development of obesity and/or diabetes (He et al., 2013; Wu et al., 2018). About 2 out of every 3 Alaskan adults are now overweight or obese (Parnell et al., 2014). The likelihood of American Indian and Alaska Native adults to have diagnosed diabetes compared with non-Hispanic whites was 2.3 times higher in 2009 (16.1% vs. 7.1%) (Department of Health and Human Services, 2012). However this correlation remains controversial as some studies suggest no such correlation between mercury and the development of metabolic syndrome (Futatsuka et al., 1996) Regardless, more investigations are needed to more fully understand the effects of MeHg on adipose tissue.

1.3 Adipose tissue

Adipose tissue (white adipose tissue) is a major endocrine system present in the human body (Figure 1.2). Initially, it was considered only for storing excess fat tissue, but now over the last decade adipose tissue has been shown to be actively involved in regulation processes (Apprahamian & Sam, 2011). Studies have shown that adipose tissue produces large amounts of biologically active and specific proteins also known as adipokines which play key roles in glucose and energy metabolism (Zhang et al., 2015a; Scherer, 2006).

Adipose tissue is made up of highly specialized cells known as adipocytes, used for the storage and release of lipids. Other cell types in adipose tissue include blood cells, endothelial cells, macrophages, pericytes and adipose precursor cells (Coelho et al., 2013). Adipose tissue and adipokines were reported to be involved in the pathogenesis of type 2 diabetes, coronary artery disease and even arthritis (Zhang et al., 2015b; Dunmore & Brown, 2012; Kohlgruber & Lynch, 2015).

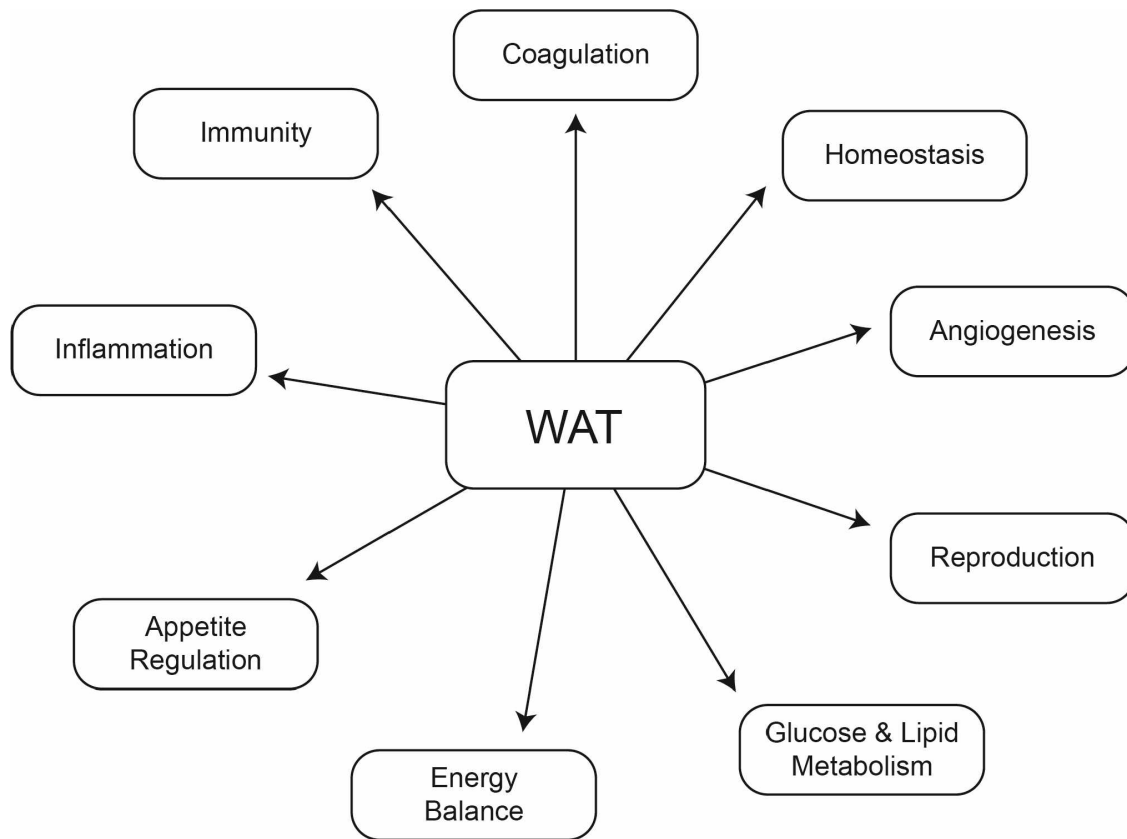


Figure 1.2: Essential biological roles exhibited by the White Adipose Tissue (WAT) (Adapted from Coelho et al., 2013)

1.4 3T3-L1 cell line

The common cell type used for in vitro studies for the phenomenon of adipogenesis and adipokines is the 3T3-L1 cell line, a well-characterized adipocyte line from mice which can acquire an adipocyte-like phenotype. During the differentiation process, 3T3-L1 cells can be induced to differentiate, under controlled laboratory conditions using a standard differentiation protocol (Figure 1.3) and are widely accepted as a physiologically faithful in vitro representation of adipogenesis (Barnes et al., 2003, 2005; Vertigan et al., 2017; Rizzatti et al., 2013).

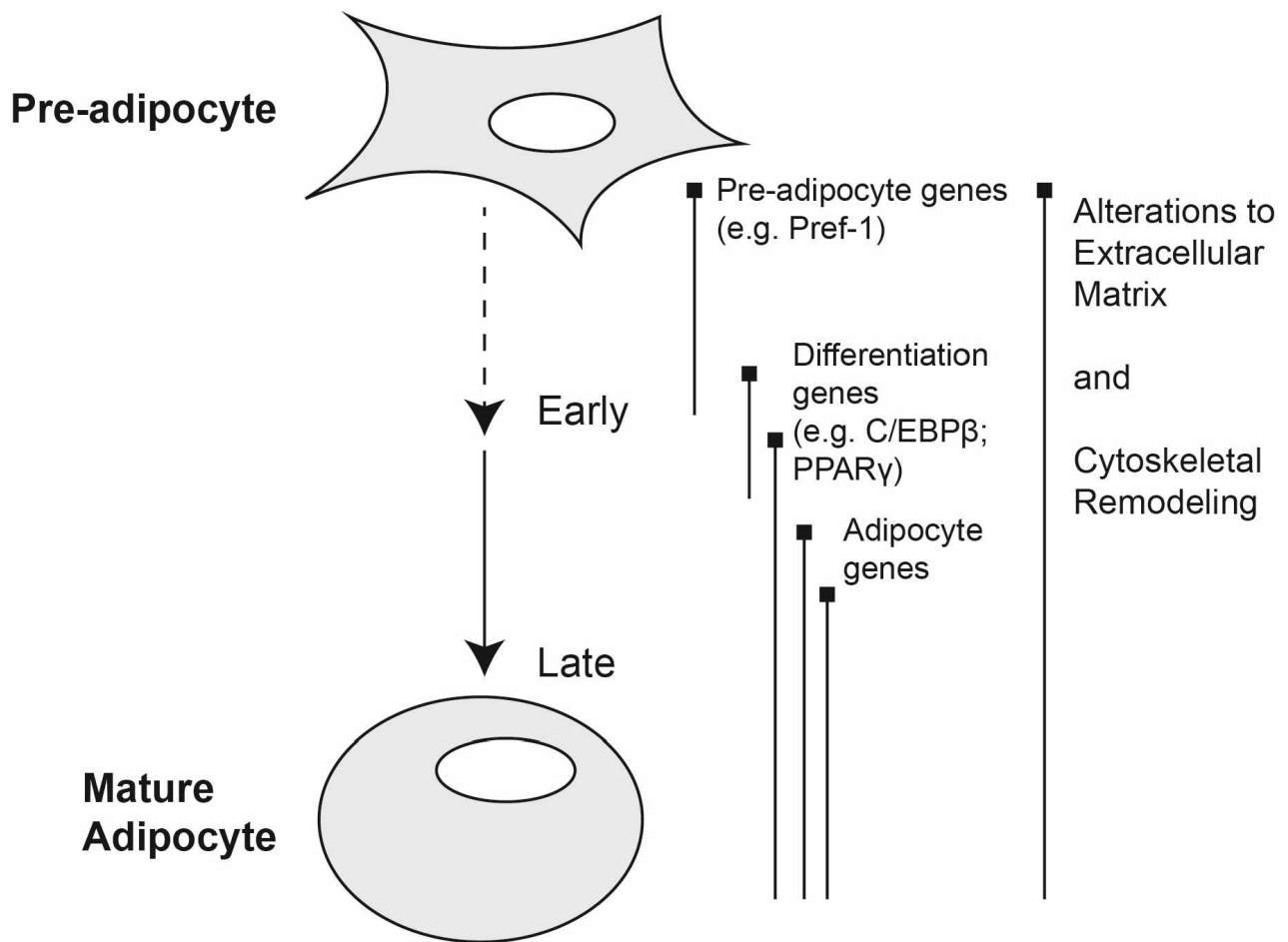


Figure 1.3: In vitro differentiation process of 3T3-L1 cell line to form mature adipocytes (Adapted from Gregoire et al., 1998)

1.5 Adipokines

Our knowledge about the functions of adipose tissue is widening over time (Figure 1.4). Adipose tissue secretes proteins generally known as adipokines to signal different functions across the body (Szendrodi, 2004; Zahorska-Markiewicz, 2006). Adipokines such as adiponectin and resistin are potential additional biomarkers for metabolic syndrome (Zhang et al., 2015a).

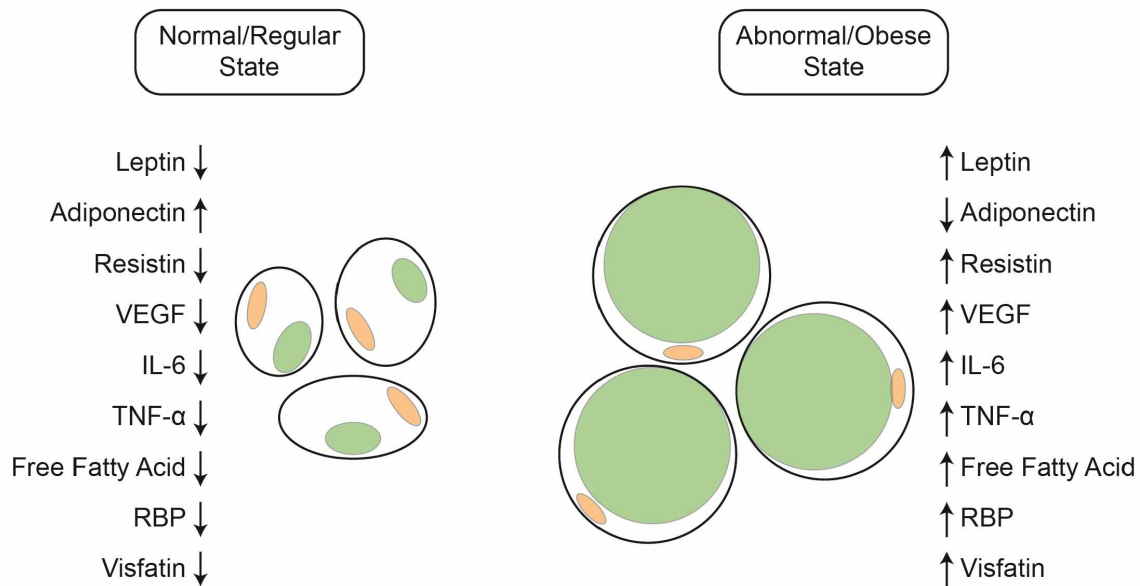


Figure 1.4: Adipokines secretion from adipocytes under normal and abnormal metabolic conditions (Adapted from Coelho et al., 2013 and Zou & Shao, 2008)

1.5.1 Adiponectin

Adiponectin is an adipokine secreted almost exclusively from the adipocytes with one of its major roles in energy metabolism (Diez & Iglesias, 2003; Koerner et al., 2005). It stimulates fatty acid oxidation, decreases plasma triglycerides and increases glucose sensitivity (Beltowski, 2003). It also acts as an anti-inflammatory, anti-atherogenic, and anti-oxidative factor (Jonas et al., 2017). Lower levels of adiponectin may lead to metabolic syndromes like insulin resistance, obesity, type 2 diabetes (Weyer, 2001; Lago et al., 2007). Higher levels may lead to anorexia nervosa (Meier, 2004). Additionally increased levels of adiponectin in chronic inflammatory diseases and other immunity mediated diseases were reported (Apprahamian & Sam, 2011). However, the validations and significance of this reported elevation of adiponectin during a state of inflammation has not been yet validated.

1.5.2 Resistin

On the other hand, resistin is a relatively new and slightly less studied adipokine with biological properties opposite to adiponectin (Beltowski, 2003; Zhang et al., 2015a). It is produced in the stromovascular fraction of adipose tissue and blood monocytes. Human resistin is 12.5-kDa protein, which contains 108 amino acids. It circulates in human blood as a dimeric protein linked by a disulfide bond. Resistin circulates in high levels in diabetic mice models (Ding et al., 2012) and it is suggested that resistin is the adipokine that links obesity to type 2 diabetes (Steppan et al., 2001; Berger, 2001). Also, resistin is an inflammatory marker of atherosclerosis in humans (Reilly et al., 2005). The adiponectin- resistin ratio has been suggested by various researchers to be an indicator of metabolic risk for obesity (Beltowski, 2003; Lau & Muniandy, 2011; Zhang et al., 2015a). The secretion levels of adipokines, like adiponectin and resistin, may be associated with risk of development of hypertension, type 2 diabetes and metabolic syndrome (Chen et al., 2006; Wu et al., 2018).

In this study, I test the hypothesis that MeHg is associated with adiponectin and resistin profiles in 3T3-L1 cells. The exposure to MeHg most likely is influenced by other stressors which need to be investigated in combination to observe any synergistic interactions of MeHg and other stressors. Pancreatic beta cells are sensitive to ROS and MeHg induces beta cell apoptosis; but, 3T3-L1 cells are less characterized (Chen et al., 2006; Guilherme et al., 2008), although apoptosis occurs in adipose tissue too. Management of adipokine levels along with antioxidants could be a useful treatment for human health programs. Using antioxidants to counteract high exposure to MeHg would be an approach to population wide studies and treatment of diabetes (Wu et al., 2017; Wu et al., 2018). A fuller understanding will facilitate the introduction of targeted diet-based interventions as treatments.

1.6 Cell model approach

Research on the effect of contaminant exposure on 3T3-L1 cells should supply baseline data and address the value of antioxidant dietary supplements as a therapeutic approach of dietary MeHg exposure on the function of adipose tissue. The roles of adipokines are numerous but we are focusing on the exacerbating role of contaminants in fat metabolism in adipose tissue. Exposure to a contaminant or mixture may lead to change in secretion patterns of adiponectin and resistin. Imbalanced ROS levels and available antioxidants have been detected in WAT of type 2 diabetics or Met S (Castro et al., 2016).

An association between mitochondrial dysfunction and oxidative stress may play critical roles in insulin resistance. High ROS levels could lead to adipocyte hypertrophy, altered metabolism, dysregulated adipokine secretion and poor apoptotic cell clearance. Basal levels of ROS are required for the differentiation of pre-adipocytes into adipocyte and their normal functioning. However, diminished or excessive levels of ROS levels may contribute to WAT dysfunction causing insulin resistance (Meo et al., 2016). Research is needed to develop models to determine the effect of a normal level of MeHg exposure on adipocytes. This understanding will add data to the debate about mercury or other contaminants and their role at the biochemical level in metabolic syndrome. Specifically, this type of research will further develop a model system to link specific environmental contaminants to metabolic syndrome and associated diseases (Magueresse-Battistoni et al., 2018; Wu et al., 2018).

Barnes and his colleagues investigated the effect of inorganic mercury chloride on adipogenesis and glucose transport (Barnes et al., 2003, 2005). Vertigan et al. showed increased VEGF secretion from differentiated cells due to MeHg exposure (Vertigan et al., 2017). Their findings provide a platform for further studying MeHg species as a potential modulator of metabolic processes in adipocytes. The idea of using a natural food in a model, anti - oxidant system to study the mitigating effects on adipokine secretion will increase the

possibility of a potential nutraceutical treatment options for insulin resistance (Wu et al., 2004). Using a defined anti-inflammatory compound would advance the current common approach of testing complex undefined extracts and mixtures (Magueresse-Battistoni et al., 2018).

In addition, as pollutants are increasing in the environment, the regulatory implications of this research would allow for fine tuning the criteria levels for water and food regulations. The few studies on complex mixtures have suggested that both additive and synergistic effects occur with multi-toxicant exposure. From a regulatory perspective, these impacts would require a review and possible lowering of the acceptable exposed dose in a food source. Studies in a standardized cell culture system allows for better comparison between toxicants.

1.7 Research Hypotheses

This study investigates four different hypothesis based on existing background knowledge. The general aim is to explore the primary effects of MeHg and TF-3 on the secretion levels of adipokines. Lipid peroxidation product, 4-HNE at the biochemical level, was used to quantify oxidative stress related to inflammation. The following hypotheses were tested using outcome measures of resistin, adiponectin and 4-HNE levels in 3T3-L1 cultures.

- a)** MeHg exposure interferes with the normal morphology of mature adipocytes resulting in distorted and clumped lipid droplets.
- b)** MeHg exposure to the mature adipocytes will change the normal secretion patterns of adiponectin and resistin.
- c)** TF-3 in a concentration dependent manner will restore the secretion patterns of adiponectin and resistin secreted from MeHg exposed adipocytes.
- d)** TF-3 concentrations will reduce the increased level of 4-HNE secreted from MeHg exposed mature adipocytes in a concentration dependent manner.

Chapter 2: Materials and Methods

2.1: Cell Culture

For the research, 3T3-L1 pre - adipocytes were purchased from American Type Culture Collection (ATCC). The thawed vial from ATCC was then subcultured using the standardized chemical induced differentiation protocol (Chemically-Induced Differentiation of ATCC® CL-173™ (3T3-L1), 2011). After 72 hours, cells were counted using a hemocytometer (Weber Scientific).

Equal number of cells (approximately 35,000 cells per 2 mL liquid medium per well), were then plated in 12-well flat-bottom cell culture plates (BD Falcon). Optimal conditions for humidified incubation of the cells were 5 % carbon dioxide along with a constant a temperature of 37°Celsius.

Triplicates of eight distinct cell populations were established. Populations were comprised of: 1) control, 2) MeHg treated and 3) MeHg + six different concentrations of theaflavin digallate (TF-3) treatments. Initially, cells were grown to 80 - 90% confluence in growth medium for 48 hours; confluent cells were then incubated for another 48 hours in the growth media. Subsequently, the cells were incubated in differentiation media for 48 hours, followed by the incubation for another 48 hours in insulin medium. Finally, all eight populations were incubated in maintenance medium for the next 10 days to obtain mature adipocytes. Before replacing or switching medium, 1.5 mL of the liquid media was collected in 2 mL eppendorf tubes and stored at - 20 °Celsius until analysis.

The concentration of MeHg used for the treatment was 100 ng/mL (0.4 µM), as we aimed to mimic the elevated blood mercury levels found in Alaskan Native populations (Hamade, 2014). It has been reported that 100 ng/mL MeHg altered VEGF secretion levels (Vertigan et al., 2017).

The effect of TF-3 on cancerous cells has been reported using different concentrations (Wu et al., 207). Similar TF-3 concentrations were used in this study to measure the effect of TF-3 on MeHg exposed 3T3-L1 adipocytes. Table 2.1 outlines eight different populations used in the study.

Table 2.1: List showing study groups of different populations

Population (All populations are plated as triplicates)	Treatment*
Population 1	Control
Population 2	100 ng/mL (0.4 μ M) MeHg
Population 3	0.4 μ M MeHg + 3.12 μ M TF-3
Population 4	0.4 μ M MeHg + 6.25 μ M TF-3
Population 5	0.4 μ M MeHg + 12.5 μ M TF-3
Population 6	0.4 μ M MeHg + 25 μ M TF-3
Population 7	0.4 μ M MeHg + 50 μ M TF-3
Population 8	0.4 μ M MeHg + 100 μ M TF-3

*Note: For populations 2 to 8, treatment started on Day 18 till Day 28. Media from Day 18 to Day 28 were stored and eventually analyzed for resistin, adiponectin and 4-HNE (Figure 2.1).

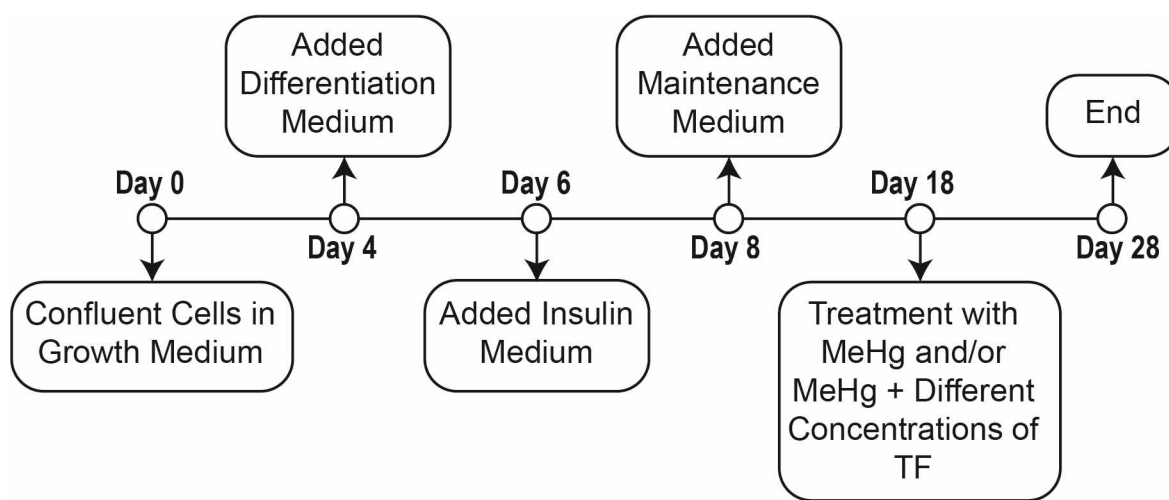


Figure 2.1: Timeline of exposure study

Table 2.2 outlines steps taken in cell differentiation process.

Table 2.2: Cell Culture Protocol

Day Name	Procedure/Medium Used
	Grow cells to confluence in Growth Medium; replace medium every 2-3 days.
Day 0	Cells are confluent. Add Growth Medium; incubate 48 hours.
Day 2	Change Growth Medium; incubate 48 hours.
Day 4	Add Differentiation Medium; incubate 48 hours.
Day 6	Add Insulin Medium; incubate 48 hours
Day 8	Add Maintenance Medium; incubate and change every 48 hours for 8-10 days until mature adipocytes are formed.
Day 18 - Day 28	Add Maintenance Medium, methylmercury (100 ng/mL) and range of concentrations of theaflavin-3,3'-digallate (3.14 μ M, 6.25 μ M, 12.5 μ M, 25 μ M, 50 μ M and 100 μ M); incubate and change every 48hours for the next 10 days.

Table 2.3 outlines chemical composition of media required for each mentioned stages.

Table 2.3: Chemical components for 3T3-L1 cell culture media

Medium Name	Chemical Composition
Growth Medium	<p>i) Dulbecco's Modified Eagle Medium (DMEM), high glucose (Sigma-Aldrich), ii) 10% calf serum (Atlanta Biologicals), 3.7 g/L sodium bicarbonate (NaHCO_3) (Sigma Aldrich), iii) 1% (by volume) penicillin/streptomycin (Gibco), and iv) 1% GlutaMax (Gibco)</p> <p>[Medium pH: 7.4]</p>
Differentiation Medium	<p>i) DMEM, high glucose, ii) 10% calf serum, iii) 3.7 g/L NaHCO_3, iv) 1% (by volume) pen/strep, v) 1% GlutaMax, vi) 0.5 mM 1-methyl-3-isobutylxanthine (IBMX) (Sigma-Aldrich), vii) 0.25 μM dexamethasone (Sigma-Aldrich), and viii) 2 $\mu\text{g/mL}$ insulin (Sigma-Aldrich)</p> <p>[Medium pH: 7.4]</p>
Insulin Medium	<p>i) DMEM, high glucose, ii) 10% FBS, iii) 3.7 g/L NaHCO_3, iv) 1% (by volume) pen/strep, v) 1% GlutaMax, vi) 2 $\mu\text{g/mL}$ insulin</p> <p>[Medium pH: 7.4]</p>
Maintenance Medium	<p>i) DMEM, high glucose, ii) 10% FBS, iii) 3.7 g/L NaHCO_3</p> <p>iv) 1% (by volume) penicillin/streptomycin and, v) 1% GlutaMax</p> <p>[Medium pH: 7.4]</p>

2.2 Treatment with toxin and antioxidant

Treatment with MeHg and theaflavin was performed for a course of ten days after cells matured (Figure 2.1, Day 18 to 28). The control cells were neither treated with MeHg nor any concentration of tea compound, TF-3, for the entire 28 day course of cell culture. MeHg treatment on 3T3-L1 adipocytes population was performed from day 18 through day 28 (population 2). Different concentrations of TF-3 (3.14, 6.25, 12.5, 25, 50 and 100 μ M) were also tested on 0.4 μ M MeHg exposed cells from day 18 through day 28 (populations 3 to 8).

MeHg stock solution was purchased from Alfa Aesar having a concentration of 1000ppm in Milli-Q water. For obtaining the final concentration of MeHg, initial dilution to 1 ppm (1000 ng/mL) was performed by adding 1.4 μ L of MeHg from stock bottle in 1.4 mL of prepared maintenance medium. To obtain the final MeHg working concentration to 100 ng/mL, 200 μ L of the diluted MeHg solution (1000 ng/mL) were added to each well having 1.8mL of maintenance medium or maintenance medium plus appropriate volumes of tea compound. Fresh solutions having MeHg and/or tea compound were made each day shortly before addition to wells. The leftover and unused solutions were discarded properly as hazardous waste.

Theaflavin digallate was purchased from LKT LABS. On arrival, the tea compound, a brick red colored powder was used to make a stock solution of 1 ppm (1000 ng/mL) in dimethyl sulfoxide (DMSO, Sigma Aldrich). Appropriate volumes of stock solution were used to obtain desired concentrations required for the treatment in each mentioned population. Table 2.4 lists the volume specifications for MeHg and theaflavin along with medium used and maintained in each well. The total liquid volume comprising MeHg and/or TF-3 along with maintenance medium was maintained 2 mL. Table 2.4 outlines the composition of populations 1 to 8, well plates.

Table 2.4: Liquid media composition of culture wells plate

Control	2000 μ L growth medium
0.4 μ M MeHg	1800 μ L growth medium + 200 μ L MeHg*
MeHg+ 3.14 μ M TF-3	1794.58 μ L growth medium + 200 μ L MeHg + 5.42 μ L TF-3
MeHg+ 6.25 μ M TF-3	1789.14 μ L growth medium + 200 μ L MeHg + 10.86 μ L TF-3
MeHg+ 12.5 μ M TF-3	1778 μ L growth medium + 200 μ L MeHg + 22 μ L TF-3
MeHg + 25 μ M TF-3	1756.56 μ L growth medium + 200 μ L MeHg + 43.44 μ L TF-3
MeHg + 50 μ M TF-3	1713 μ L growth medium + 200 μ L MeHg + 87 μ L TF-3
MeHg +100 μ M TF-3	1626 μ L growth medium + 200 μ L MeHg + 174 μ L TF-3

* MeHg positive control

An EVOS XL Core Imaging System, a transmitted light microscope, was used to view cells and capture their images. Cells were imaged before changing and replacing culture medium. Control cells were imaged from Day 0 to Day 28 and treated cells were imaged from Day 18 to Day 28. “Day 2” images represent the appearance of the cells after 48 hours of incubation with Growth Medium, “Day 4” images show cells after 48 hours in Differentiation Medium, and so on (Figure 2.1).

2.3. Safety

Appropriate personal protective equipment was used at all times while working with MeHg solutions. Silver Shield gloves, along with an additional outer nitrile glove were worn, whenever concentrated MeHg stocks were opened, as well as disposable lab coats and a chemical safety hood. All mercury-containing liquid or solid wastes, including cell media, Falcon tubes,

Eppendorf tubes, and pipet tips, were disposed of as hazardous waste according to local regulations.

2.4. Morphology: Lipid (Oil Red O) Staining

A Lipid staining kit was used for selective staining and detection of lipid droplets in matured 3T3-L1 cells (matured adipocytes). Oil red O is a lysochrome diazo dye used for staining lipids. Hematoxylin included in the kit stains the nuclei of the cells. The Lipid (Oil Red O) Staining Kit contained PBS, 10% formalin, Oil Red O and hematoxylin (Sigma Alrich). Other reagents and reagents required were Whatmann No. 1 filter paper, 60 % isopropanol and 100% isopropanol. The experimental protocol is briefly described below:

On Day 28 of cell culture, immediately after the media collection from all the wells, cells were ready for staining. The staining assay started with the remaining cell culture media in the wells being removed. After removal of cell culture media, cells were washed twice with PBS. After the wash, 10% formalin was pipetted down on to the sides of wells. The formalin treated cells were incubated for 45 minutes.

After the incubation period, formalin was discarded and cells were washed twice with water. 60% isopropanol was added to wells and incubated for 5 minutes. After discarding the 60% isopropanol, cells were evenly covered with Oil Red O working solution (was prepared 15 minutes before use by adding, mixing and filtering 3 parts of Oil Red O stock solution to 2 parts of water).

The well plate was gently rotated and incubated for 15 minutes. After the incubation period, the Oil Red O solution was discarded and stained cells were washed five times with water until no excess stain was seen. After obtaining clear cells, hematoxylin was added on to the cells and was incubated for 1 minute. After which, hematoxylin was discarded and cells were washed five times with water. Cells were covered with water and observed under a

microscope. Images were captured at the time of observation. Lipid droplets appeared red and nuclei appeared blue.

2.5 Enzyme Linked Immunosorbent Assay (ELISA)

The Enzyme Linked Immunosorbent Assay (ELISA) is a highly specific and sensitive technique used for quantitatively determining the analyte or protein of interest in a given biological sample. It works on the principle of specific binding of an antigen to its antibody. There are different types of ELISA kits available in the market based on the type of antigen-antibody binding; the most commonly used principle is “sandwich ELISA”. Another principle type also used in this study is “competitive ELISA”. The analytes of interest in this study were adiponectin, resistin and, 4-Hydroxynonenal (4-HNE). Commercially available ELISA kits were purchased from R & D Systems, and MyBioSource, respectively.

A schematic below adapted from technical information portal of R&D systems describes the principle of sandwich and competitive ELISA.

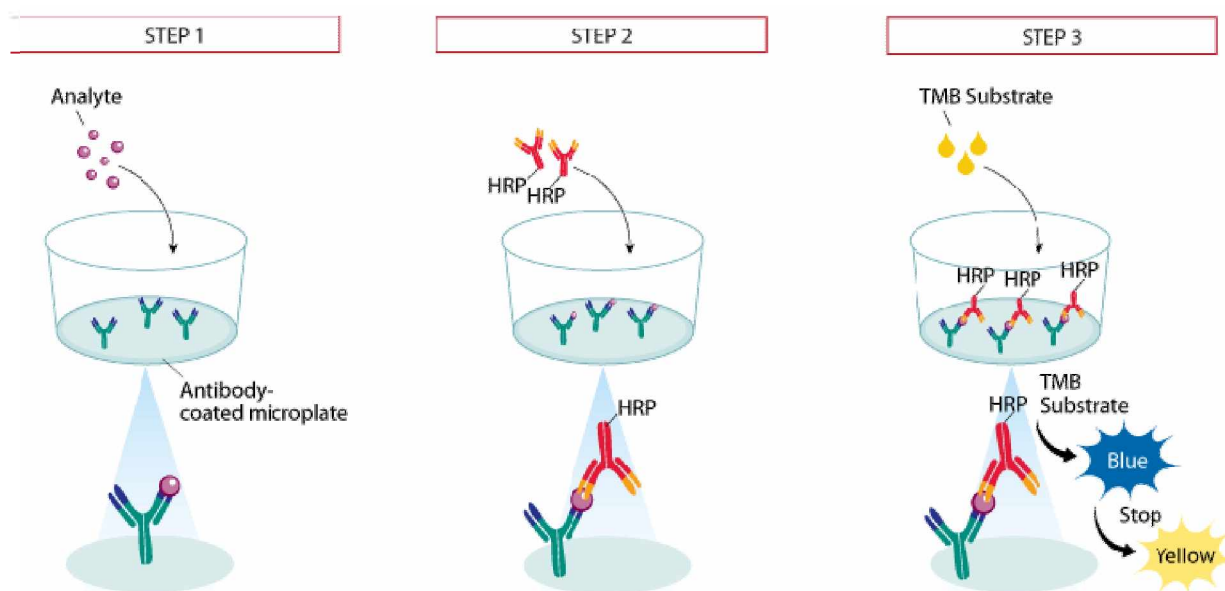


Figure 2.2: Schematic of basic sandwich ELISA technique
(Source: Colorimetric Sandwich ELISA, R&D Systems)

In the sandwich ELISA, a provided microplate is pre-coated with a specific monoclonal antibody (Figure 2.2). Upon addition of the set of standards, control and samples using a pipette, the analyte of interest binds with the pre-coated capture antibody. After incubation for 2 to 3 hours period, microplate is rinsed, resulting in the washing away of unbound antigen and other materials. An enzyme-linked polyclonal detection antibody also specific to a different epitope on the analyte of interest is pipetted into the wells of microplate, in order to bind captured antigen or analyte of interest. After the incubation, the wells are rinsed and unbound materials are washed away. A substrate solution is added to the wells and there will be a generation of blue colored solution; the intensity of the blue color is directly proportional to the concentration of the analyte of interest present in the biological sample. To stop the ongoing chromogenic reaction, a sulfuric acid stop solution is added to the wells turning blue colored solutions to yellow. The absorbance reading is then recorded at 450nm for the standards' and samples' absorbance values. A standard curve having concentrations of antigen as the X-axis is then generated, for further interpolating the unknown concentration of the analyte of interest in samples based on the obtained reading.

In competitive ELISA, a microplate provided has been pre-coated with a known and specific antigen to which samples containing unknown concentrations of antigen and standards having the known concentrations are added. Immediately after, the biotinylated labeled antibody, which is specific for the targeted antigen, is added to the wells containing samples and standards. After incubating for a specific period of time, the plate is rinsed several times with the wash buffer removing all the unbound samples or conjugate. Then horseradish peroxidase (HRP) conjugated to avidin is added to the wells and incubated for a certain period of time. After reacting with HRP, followed by another set of rinse with wash buffer, substrate solution is added to wells. The reaction between the enzyme and substrate formed a colored solution. To stop the ongoing reaction, stop solution is added to the wells and the absorbance readings were

recorded using a spectrometer at 450 nm. The concentration of the antigen in the samples can be interpolated by the equation obtained by the standard curve.

The key step in this process is a competitive interaction of sample antigen or antibody to labeled antibody or antigen which is in limited concentration respectively. The obtained signal output is inversely proportional to the concentration of antigen in a sample where there is an output of a weaker signal at higher concentration of antigen.

2.5.1: Sandwich ELISA: Adiponectin

The kit used was R&D Systems's Quantikine Mouse Adiponectin ELISA .The kit provides its own protocol, which is described briefly below:

The frozen cell media from different population were thawed at room temperature, after which, the thawed eppendorf tubes containing cell media were centrifuged at 2000 rpm for five minutes to remove particulates. The kit provided a known adiponectin standard which was serially diluted to generate a standard curve. The possible adiponectin detection range was 0 ng/mL – 10 ng/mL. The samples were diluted to 1/3 with calibrator diluent before loading them into ELISA microwell plate. The purpose of sample dilution was to obtain absorbance readings within the known standard curve. 50 μ L of standards, blank and diluted samples were added to the adiponectin antibody coated microplate, followed by microplate incubation for 3 hours at room temperature, after which, the microplate got rinsed five times using wash buffer. Later, 100 μ L of conjugate antibody was added to the microplate and the plate was incubated for another one hour at room temperature. The microplate was again washed five times with wash buffer after which 100 μ L of substrate solution was added to the plate and incubated for another 30 minutes in the dark. The last step of the process was the addition of the stop solution which generated a yellow color; the absorbance was read at 450 nm in a BioTek Synergy HT plate reader using Gen5 software (Figure 2.3).

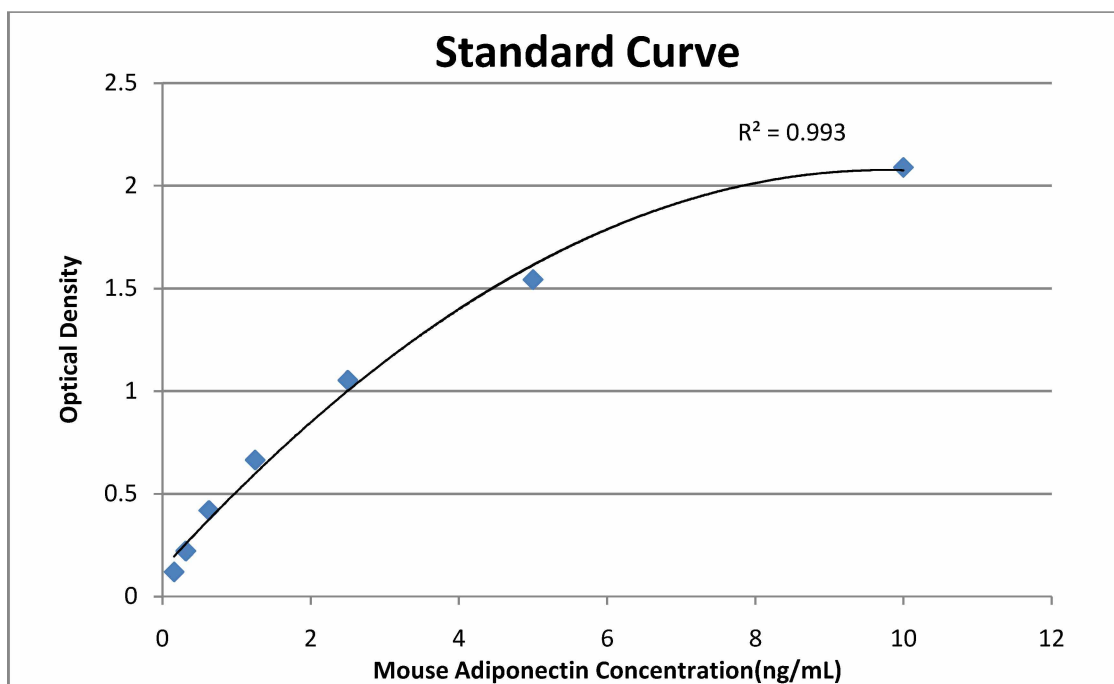


Figure 2.3: Adiponectin Standard Curve

2.5.2: Sandwich ELISA: Resistin

The kit used was R&D Systems's Quantikine Mouse Resistin ELISA .The kit provides its own protocol, which is described briefly below.

Frozen cell media from different population were thawed at room temperature. After which, the thawed eppendorf tubes containing cell media were centrifuged at 2000 rpm for five minutes to remove particulates. The Kit provided a known resistin standard which was serially diluted which was used to generate a standard curve. The possible resistin detection range was 0 pg/mL – 2000 pg/mL. The samples were diluted to 1/3 with calibrator diluent before loading them into ELISA microwell plate.

The purpose of sample dilution was to obtain absorbance readings within the known standard curve. 50µL of standards, blank and diluted samples were added on to the resistin

antibody coated microplate, following microplate incubation for 2 hours at room temperature on a horizontal microplate shaker set at 500 rpm.

After which, the microplate was rinsed five times using wash buffer. Later, 100 μ L of conjugate antibody was added to the microplate and the plate was incubated for another two hours at room temperature. The microplate was again rinsed five times with wash buffer after which 100 μ L of substrate solution was added to the plate and incubated for another 30 minutes in the dark. Similar to adiponectin ELISA, the last step of the process included the addition of the stop solution which generated a yellow color; the absorbance was read at 450 nm in a BioTek Synergy HT plate reader using Gen5 software (Figure 2.4).

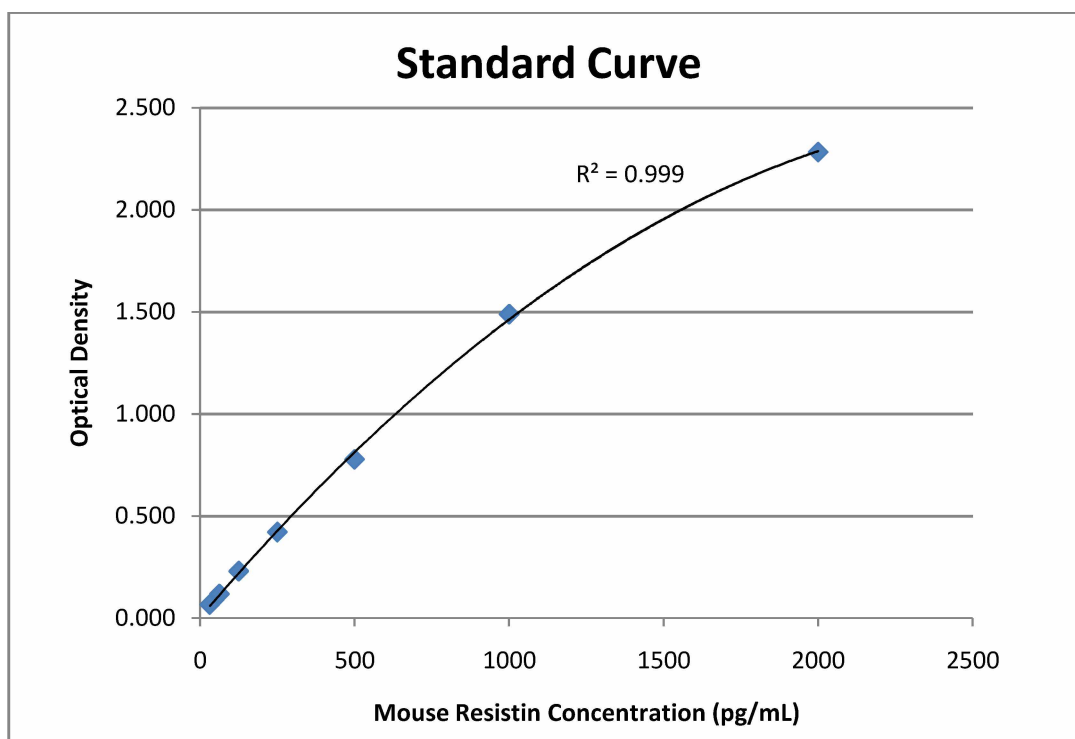


Figure 2.4: Resistin Standard Curve

2.5.3: Competitive ELISA: Mouse 4-Hydroxynonenal (4-HNE)

The kit used was MyBioSource's Quantikine Mouse 4-Hydroxynonenal (4-HNE) ELISA. The kit provides its own protocol, which is described briefly below.

Frozen cell media from different population were thawed at room temperature. After which, the thawed eppendorf tubes containing cell media were centrifuged at 2000 rpm for five minutes to remove particulates. A Kit provided a known 4-HNE reference standard which was serially diluted which was used to generate a standard curve. The possible 4-HNE detection range was 0 ng/mL – 100 ng/mL. The samples were diluted to 1/2 with sample diluent before loading them into ELISA microwell plate. The complete experiment was performed at 37°Celsius.

50 µL of standards, blank and diluted samples were added on to the 4-HNE antigen coated well plate. Immediately, 50 µL of Biotinylated detection antibody was added to the well plate which was later sealed and incubated for 45 minutes at 37°C. After which, the microplate got rinsed three times using wash buffer. 100 µL of HRP conjugate solution was added to the microplate and the plate was incubated for another 30 minutes at 37°C. The microplate was again rinsed five times with wash buffer after which 90 µL of substrate solution was added to the plate and incubated for about minutes in the dark. Similar to adiponectin and resistin ELISA, the last step of the process included the addition of the stop solution terminating the ongoing enzyme substrate reaction; the absorbance was read at 450 nm in a BioTek Synergy HT plate reader using Gen5 software (Figure 2.5)

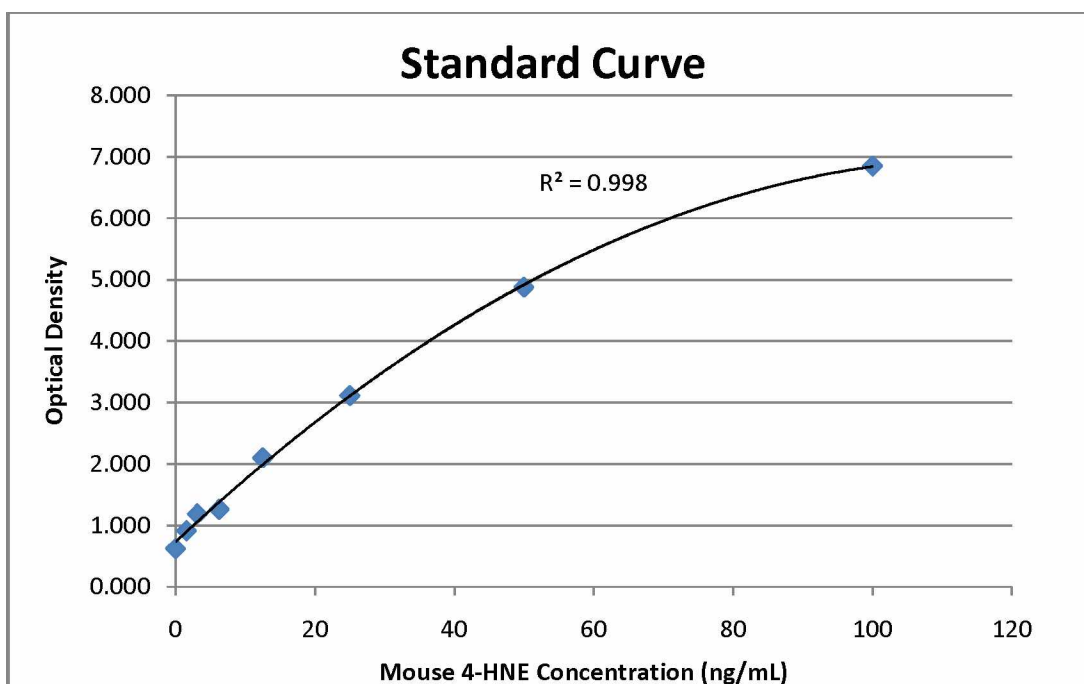


Figure 2.5: 4-HNE Standard Curve

2.6 Statistical analysis

The cell culture setup included triplicates of each population (population 1 to 8). Graphpad Prism, version 8.0.1 software was used to prepare all the plots and to perform statistical analyses. For analyzing the adipokines and 4-HNE levels, cell culture media was collected from Day 0 to Day 28. However, for the analysis of adipokines and 4-HNE secreted from the treated populations (population 2 to 8) cell culture media was collected from Day 20 to Day 28. The samples were collected at a regular interval of 48 hours.

The normal secretion patterns of adipokines and 4-HNE will be represented by line charts and/ or bar graphs, comprising values of mean \pm standard deviation obtained from three different experiments. Each day (from Day 0 to Day 28) had three values or data points, which were averaged to obtain mean values and to calculate standard deviation.

To determine the statistically significant difference between the secretion levels of adiponectin, resistin and 4-HNE from the non- treated and treated cell populations, overall effect was considered instead of effect on a single day. Three replicates from each day (Day 20, Day 22, Day 24, Day 26 and Day 28) were analyzed collectively, each population had a total of 15 data points (n=15), comprising values obtained from three different experiments.

To determine the normality of the data, Shapiro Wilk test was used. Normally distributed data were analyzed using parametric tests. To determine the overall statistical significance, one way analysis of variance (ANOVA) was applied. Values were found to be statistically significant different if the p-value was less than 0.05.

To determine the significant difference between two populations, (e.g. control cells vs. MeHg treated cells or control cells vs. MeHg+ 3.14 μ M theaflavin and so on), Student's T test was used, and data were found to be significant if the p-value was less than 0.05. In order to correct for multiple comparisons, Bonferroni corrections were performed on all T - tests.

Non-normal data were analyzed using non parametric methods. To determine the overall statistically significance, Kruskal–Wallis one-way analysis of variance was applied. Values were found to be statistically significant if the p-value was less than 0.05. However, to determine the significant difference between two populations, (e.g. control cells vs. MeHg treated cells or control cells vs. MeHg+ 3.14 μ M theaflavin and so on), Mann–Whitney U test was used and data were noted to be significant if p-value was less than 0.05. Similarly, in order to correct multiple comparisons, Bonferroni corrections were performed on all pairs of columns.

Data are presented as mean \pm standard deviation unless indicated otherwise. Alpha value was taken as 0.00625 instead of 0.05 after Bonferroni correction. Differences were considered significant (*) if p-value is less than or equal to 0.00625, very significant (**) if less than or equal to 0.001 and extremely significant (***) if less than or equal to 0.0001.

Chapter 3: Results

3.1 Morphological changes

3.1.1. Morphological changes in 3T3-L1 cell line to form mature 3T3-L1 adipocytes

Morphological changes were followed from day 2 to day 28, from day 18 to day 28.

Morphological changes in MeHg and TF-3 treated cell populations were studied from day 18 to day 28.

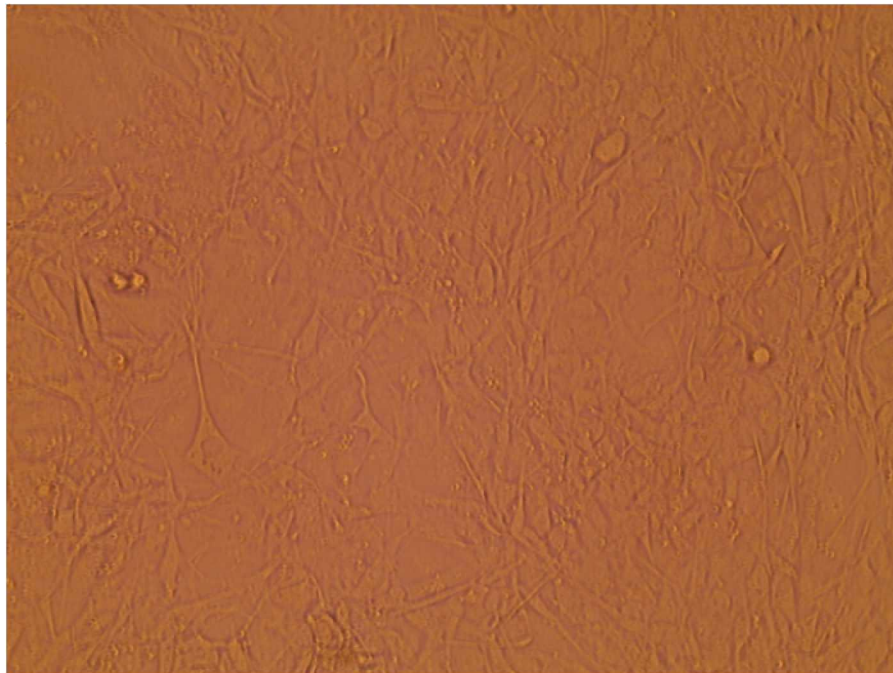


Figure 3.1a: 3T3-L1 pre-adipocytes (Day 2). Adipocytes start out as pre-adipocytes with general fibroblast morphology. Figure 3.1a shows an image of cells on day 2. The morphology exhibited is that of fibroblasts, flat and elongated. Pre-adipocytes at this stage of cell culture are growing in growth medium. This image shows a confluence of 80-90%, prior to differentiation. There is no such spherical phenotype seen.

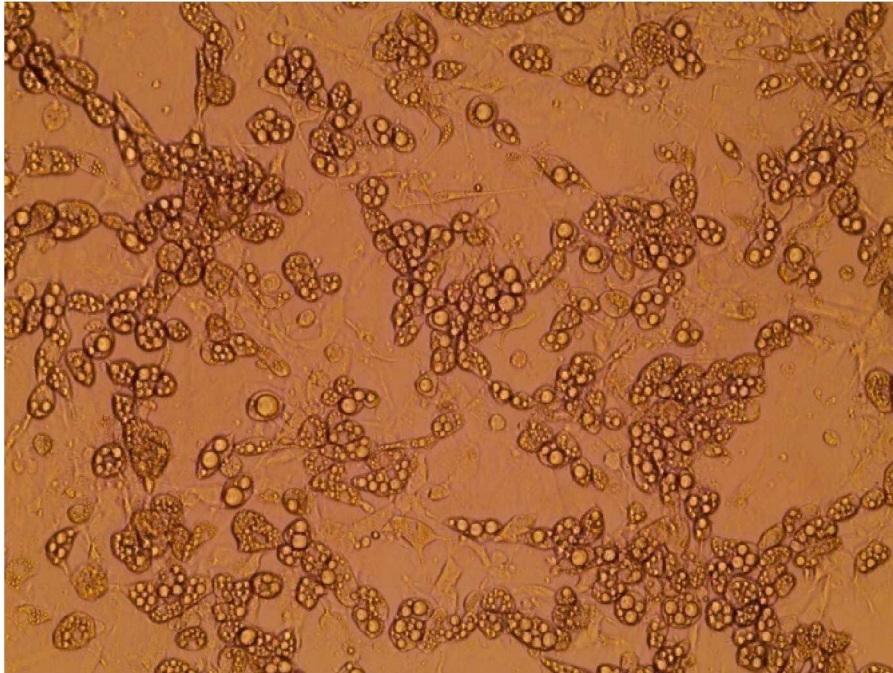


Figure 3.1b: 3T3-L1 differentiating adipocytes (Day 18). After exposure to chemical signals, the pre-adipocytes are transformed to a spherical morphology. Fig 3.1b shows an image of cells on day 18. The morphology exhibited is spherical, in the form of lipid droplets. Pre-adipocytes have been grown in accordance to tables 2.2 and 2.3. Elongated morphology is now replaced with more prominent spherical cells consisting of lipid droplets. Not of all these cells have differentiated completely; they are still in process of differentiation. However, they are growing in maintenance medium. Treatment started from this day, day 18. Fat globules are visible.

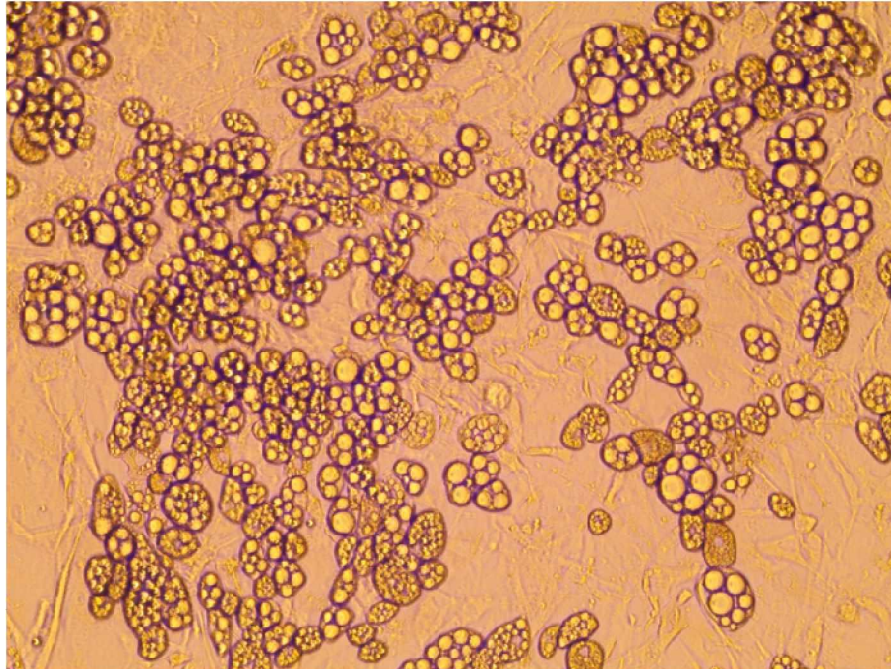


Figure 3.1c: Mature 3T3-L1 adipocytes (Day 28). At day 28, the fat droplets have enlarged. Fig 3.1c shows an image of cells from last day of the study, day 28. The morphology exhibited is of mature, spherical, adipocytes with more prominent and visible lipid droplets. It can be seen that there are additional significant phenotypical changes in terms of lipid droplets. However, cellular apoptosis starts occurring at this point and the cell number started to decrease. Adipokines are secreted from both the differentiating and differentiated mature adipocytes. This stage shows the increase in the size of fat droplets.

3.1.2 Morphological changes in 3T3-L1 adipocytes on Day 20 upon exposure to MeHg and TF-3)

Figure 3.1d shows detailed images captured before replacing the maintenance medium at Day 20 of the cell culture study. At day 18, 100 ng/mL (0.4 μ M) MeHg was added to populations of 3T3-L1 adipocytes. This figure shows the control, MeHg and different concentrations of TF-3 after exposure. Variations in the size of the fat droplets in the MeHg exposed population can be seen.

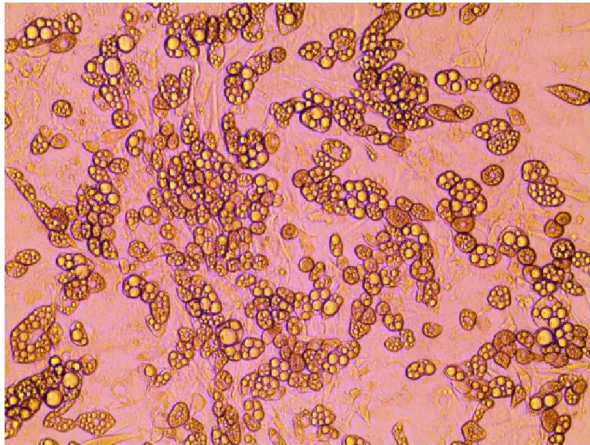
Population 1 shows a healthy set of confluent adipocytes. Most of the developed cells have attained a spherical round shape suggesting that the cells have attained more vivid and visible lipid droplets. Control cells on Day 18 (Figure 3.1b) were less confluent and lesser cells had round shape as compared to day 20. No such unexpected phenotypic change was seen at this point of the qualitative observation of cells. However, population 2 shows a set of cells exposed to 100 ng/mL MeHg. Lipid droplets are quite different from the control cells. It seems that half of the cells appeared to have attained a sac like structure and the cell number seems to have decreased which was expected as this is probably due to increase in free radical stress. Developing or differentiating cells in the background are not visible suggesting the beginning of cellular apoptosis, caused by increased stress or an imbalance in redox conditions.

Population 3 shows treatment with 3.14 μ M TF-3, along with 100 ng/mL (0.4 μ M) MeHg. Cells look healthier than population 2 in terms of appearance and number of lipid droplets, however the droplet size is less similar to the control cells, some distorted and clumped lipid droplets can also be seen. Furthermore, a qualitative analysis of population 4 showed that the treatment of 6.25 μ M TF-3 along with MeHg resulted in most of the lipid droplets attaining a turbid appearance resulting in opaque droplets. The reason for this change was not known, but might be due to apoptosis. The increased tea concentration results in apoptosis of the MeHg damaged cells. Cell numbers appear to decrease.

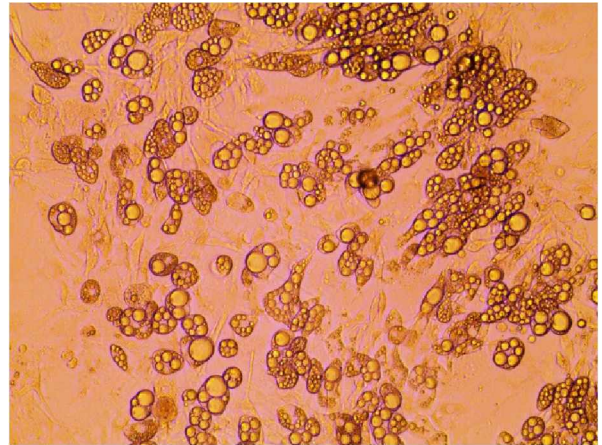
In contrast to populations 3 and 4, population 5 consisting of treatment with 25 μ M TF-3, with MeHg, looked similar to control cells however, cell murkiness is still present and visible. Decreasing cell number continues in this population too. Population 6 showed similar smaller size of lipid droplets as seen in population 5, cell clumping was also seen as well as the murky/turbid cell texture.

In population 7, which had cells treated with 50 μ M TF-3, along with MeHg, the droplets showed some oil droplets hanging on the water surface with no definite adipocytes shape. I suggest that the cells definitely were distorted along with a murky background which could be

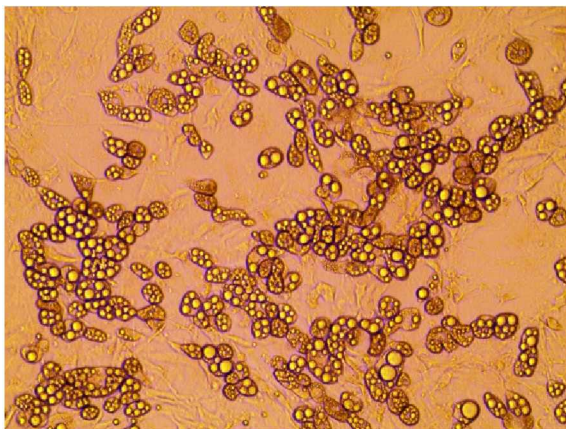
due to higher concentration of tea stimulating apoptosis. Lastly, Population 8 showed a highly increased loss of cells compared to control. Remaining lipid droplets looked unhealthy and appeared to have attained small granular shape instead of a visible and definite round shape seen in the control population.



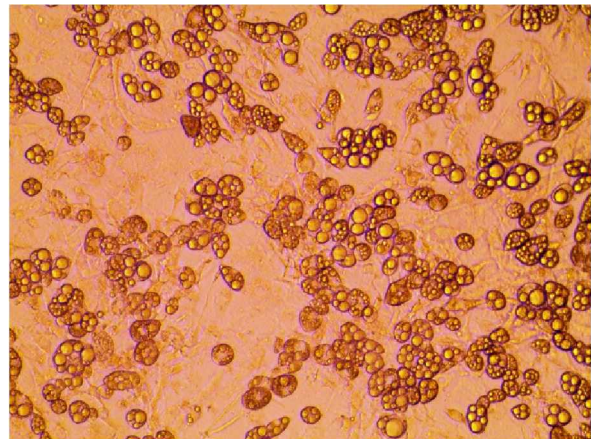
Population 1: Control



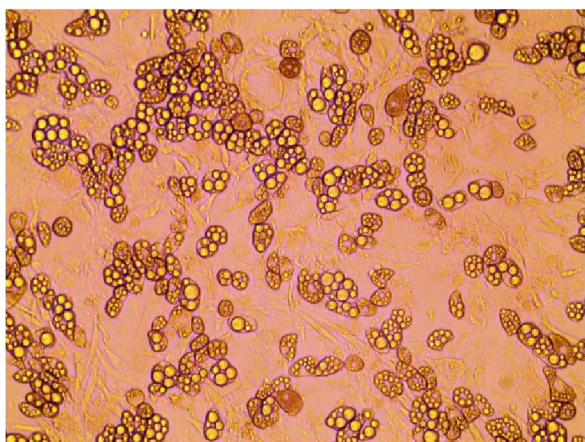
Population 2: MeHg



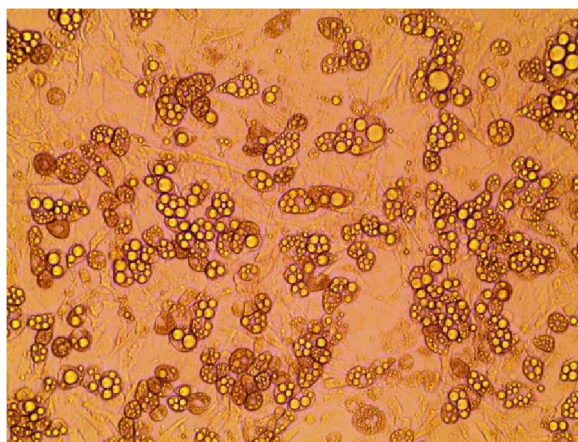
Population 3: MeHg + 3.14 μ M TF-3



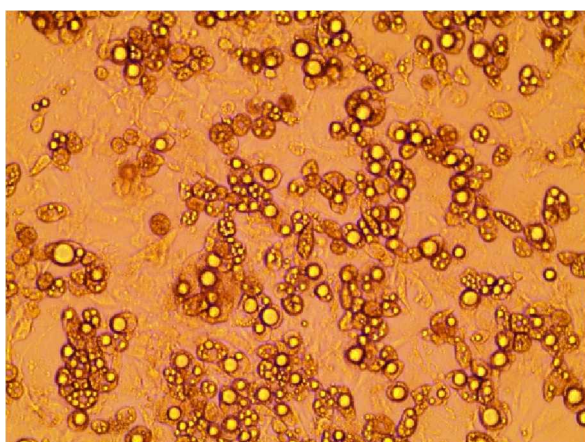
Population 4: MeHg + 6.25 μ M TF-3



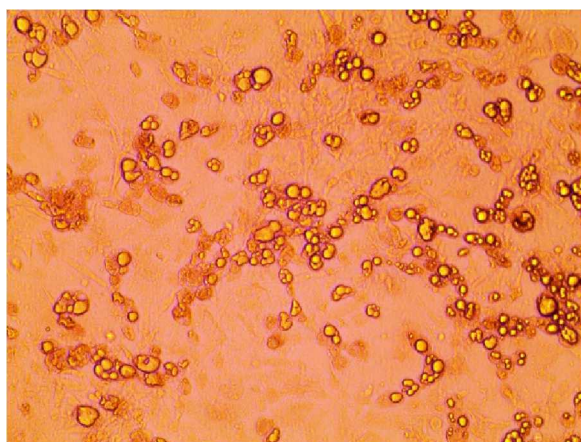
Population 5: MeHg + 12.5 μM TF-3



Population 6: MeHg + 25 μM TF-3



Population 7: MeHg + 50 μM TF-3



Population 8: MeHg + 100 μM TF-3

Figure 3.1d: Morphology changes caused due to different treatments to mature adipocytes on Day 20.

3.1.3 Morphological changes in 3T3-L1 adipocytes on Day 22 upon exposure to MeHg and TF-3.

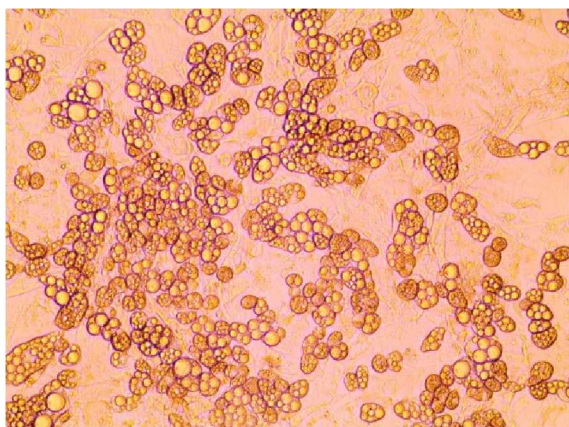
Figure 3.1e shows later set of images of the control and treated adipocytes at day 22.

Population 1, the control, contains more rounded cells having developed lipid vesicles or lipid droplets. The overall impression is the presence of greater percentage of differentiated cells. It

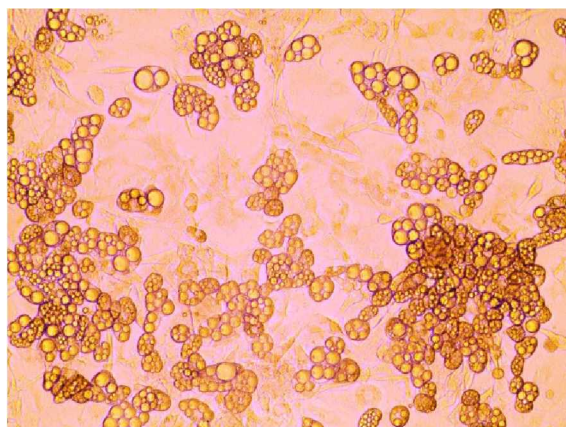
also cells appear to have grown uniformly over the culture plate surface. Population 2 exhibits the different morphology of the adipocytes suggesting the stressed pattern. Cells are spherical in shape but are highly clumped with other surrounding cells; and, some cells are distorted in shape, compared to the control cells (population 1). Also, some groups of agglomerated cells can also be seen on one side of the plate suggesting abnormal growth due to MeHg caused stress.

Cells in population 3 look better than cells in population 2 in terms of showing overall normal appearance of cell morphology. MeHg (population 2) may have caused increased change in the cell redox state which led to the abnormal shape and size of cells, but in population 3, cells contain lipid droplets in spite of having surrounded by distorted cells. Cell growth distribution looks uniform in population 4, however, adipocytes/cells size look smaller as compared to control cells. Much cell clumping can also be seen. Cells in population 5 look similar to population 4 in terms of overall appearance and size of cells; however, cell distribution is highly dispersed when compared to the control group. Higher scattering of cells can be observed in population 6 along with smaller cells number as compared to the control group. Higher cell clumping can again be seen which could lead to further cell death.

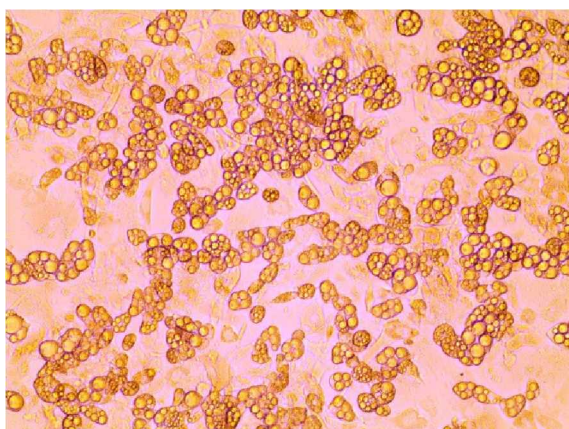
Population 7 cells' seem to have bigger lipid droplets with less clumping but cell number looks comparatively smaller than control cells. The appearances of some cells in population 7 are greatly different from other treated groups. Greater difference in cell morphology can be seen in population 8, where higher scattering of cells can be seen with absolute lesser number of cells.



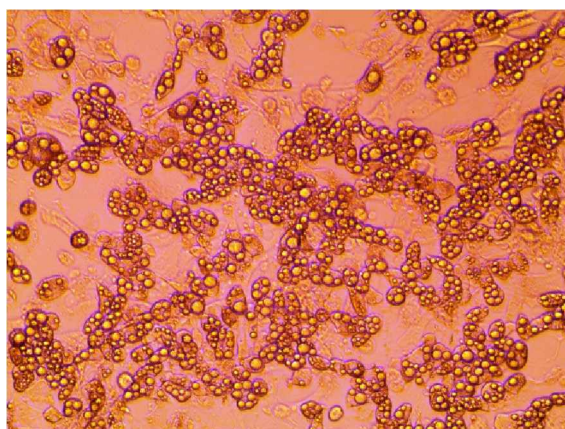
Population 1: Control



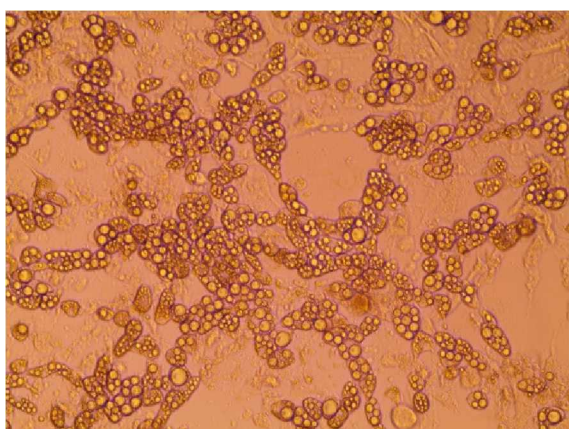
Population 2: MeHg



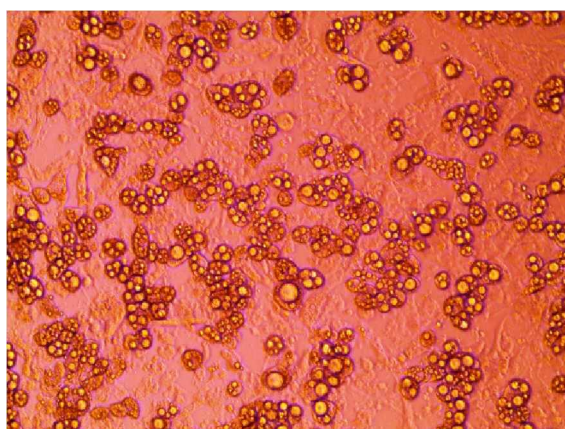
Population 3: MeHg + 3.14 μ M TF-3



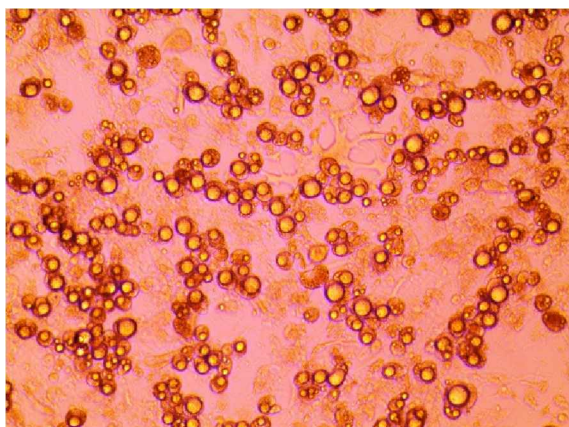
Population 4: MeHg + 6.25 μ M TF-3



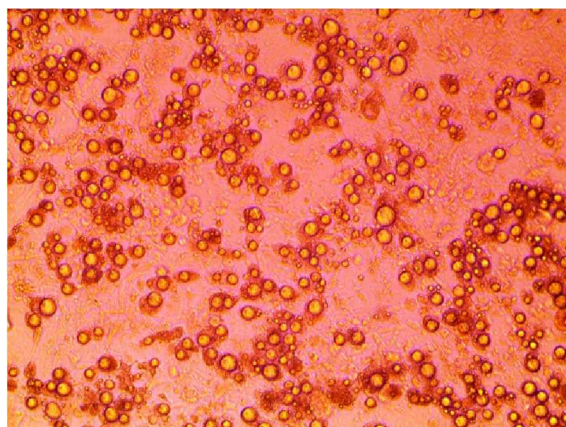
Population 5: MeHg + 12.5 μ M TF-3



Population 6: MeHg + 25 μ M TF-3



Population 7: MeHg + 50 μ M TF-3



Population 8: MeHg + 100 μ M TF-3

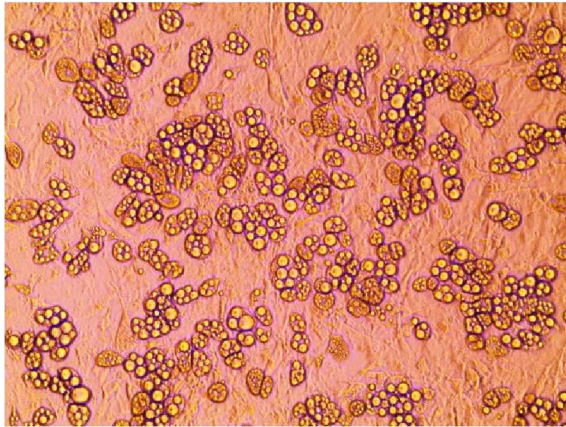
Figure 3.1e: Morphology changes caused due to different treatments to mature adipocytes on Day 22.

3.1.4 Morphological changes in 3T3-L1 adipocytes on Day 24 upon exposure to MeHg and TF-3.

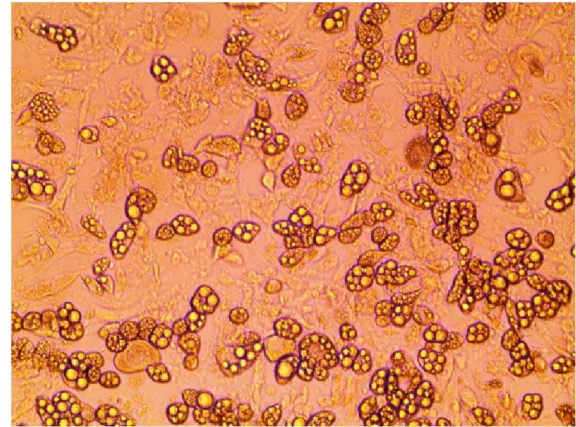
Figure 3.1f shows a detailed set of images of cell populations taken at day 24. Cells in the control group of population 1 maintained a rounded shape and have lipid droplets in them. However, the overall cell number looks slightly less than days 20 and 22, resulting from general apoptosis which is expected at day 24 of the cell culture study. Cells are still growing and maintaining their spherical, normal cell morphology. MeHg exposed cells in population 2 are smaller in number, higher number of groups of agglomerated cells. Cell death is quite visible due to MeHg induced stress.

Appearance of cells in population 3 is different; some murkiness/turbidity can be seen around cells. Cells number is greater than population 2 but some cells in population 3 look unhealthy and distorted unlike those observed on day 22. Most of the cells in population 4 are spherical in shape and seem to contain smaller lipid droplets. Higher cell clumping can be seen and slight murkiness over the upper half of the plate.

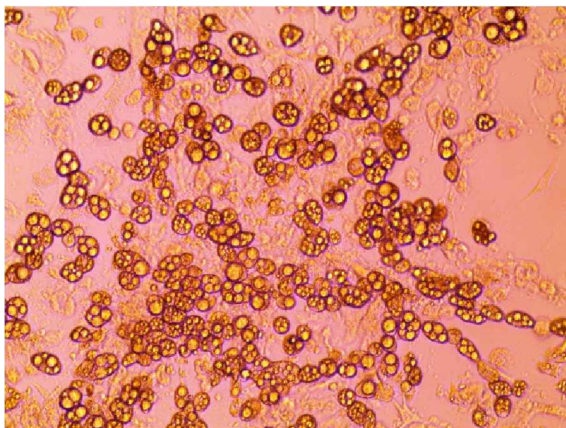
Populations 5 and 6 look quite similar in terms of having smaller sized cells, scattering of cells with several mini groups of clumped cells. Little dullness can be seen in cells which might suggest a stress environment induced by MeHg exposure. Different morphologies of cells can be seen in population 7 and 8 along with less number of cells with higher scattering and few remaining healthy adipocytes.



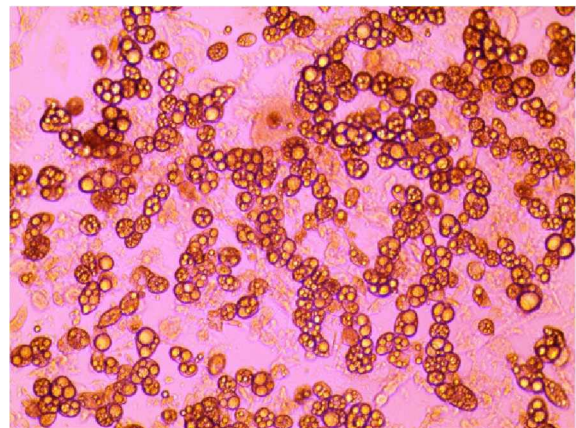
Population 1: Control



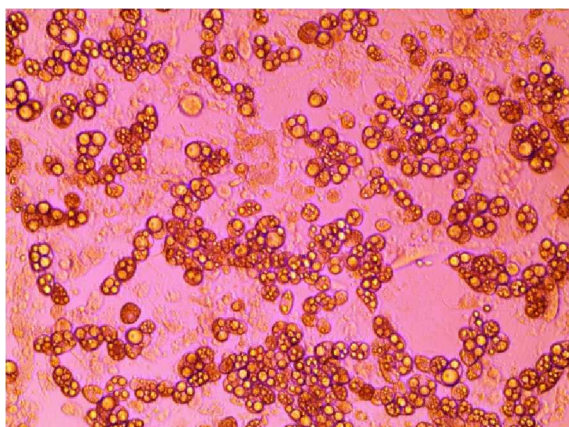
Population 2: MeHg



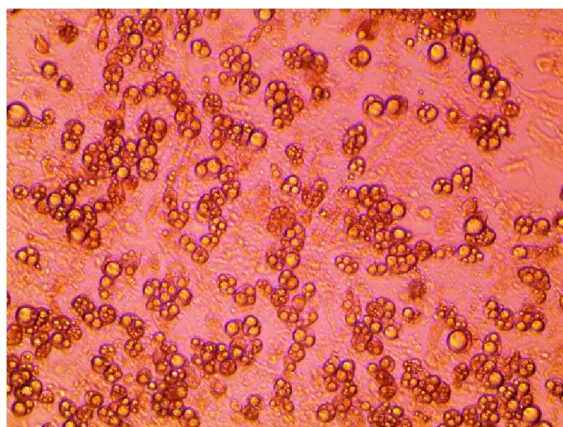
Population 3: MeHg + 3.14 μ M TF-3



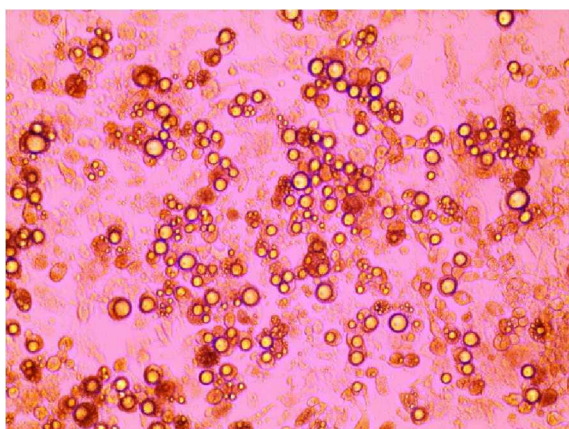
Population 4: MeHg + 6.25 μ M TF-3



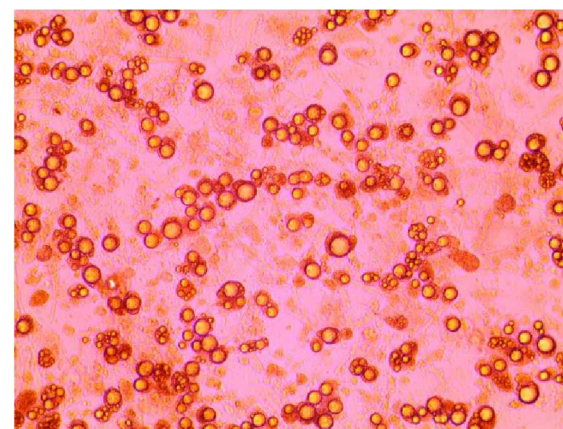
Population 5: MeHg + 12.5 μ M TF-3



Population 6: MeHg + 25 μ M TF-3



Population 7: MeHg + 50 μ M TF-3



Population 8: MeHg + 100 μ M TF-3

Figure 3.1f: Morphology changes caused due to different treatments to mature adipocytes on Day 24.

3.1.5 Morphological changes in 3T3-L1 adipocytes on Day 26 upon exposure to MeHg and TF-3.

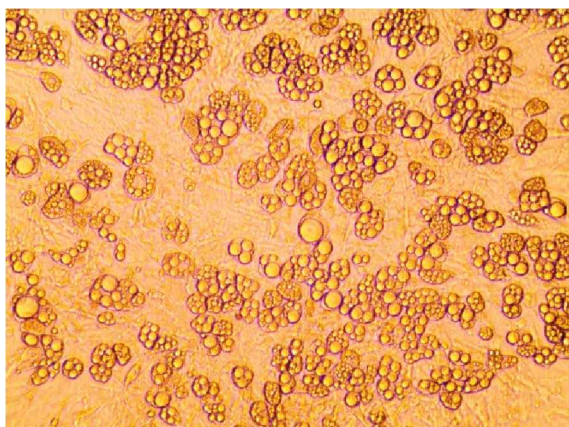
Figure 3.1g shows a set of images of the control and treated cell populations on day 26.

Population 1 continues to show healthy spherical cells; the number of cells has increased from day 24. Cells are uniformly distributed having definite lipid droplets showing successful cell differentiation. No other noticeable change can be seen. However, cells in MeHg exposed population 2 look highly abnormal, murkiness can be seen around MeHg exposed distorted

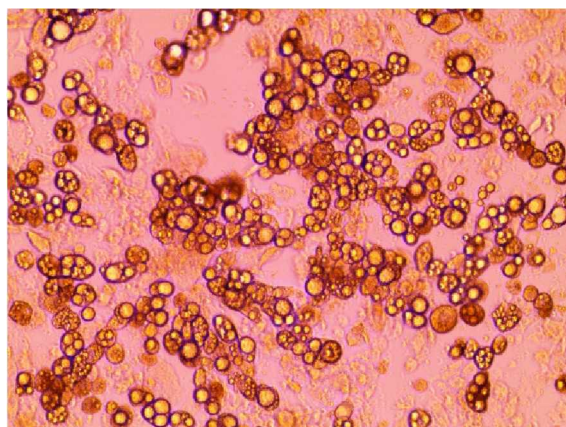
cells. In the center of the image, an unhealthy clump of cells can also be argued to point out distorted cells or murkiness suggesting stress in the environment.

Despite the exposure of MeHg, cells in population 3 maintained similar sizes and shapes of lipid droplets as the control cells, suggesting some affect from TF-3 concentration to improve or maintain the standard cell morphology of adipocytes. The cell number is smaller when compared to control group but the phenotypical similarity is quite comparable to the control cells in population 1. In population 4 on day 26, it seems that 6.25 μ M TF-3 has not done much to maintain the spherical morphology of cells. A translucent appearance could be observed at the center of the image. Some cells are not visible in some part, mostly because they are overshadowed with some cell debris or some other cell secretion. Cells in population 5 appeared similar to population 4. Cells are fewer in number but shape and size look quite similar to control cells; however a column of clumped cells formation can also be seen. On the other hand, TF-3 concentration in population 6 is an inappropriate concentration to maintain the cell morphology. Most of the cells seem to be dead at this point.

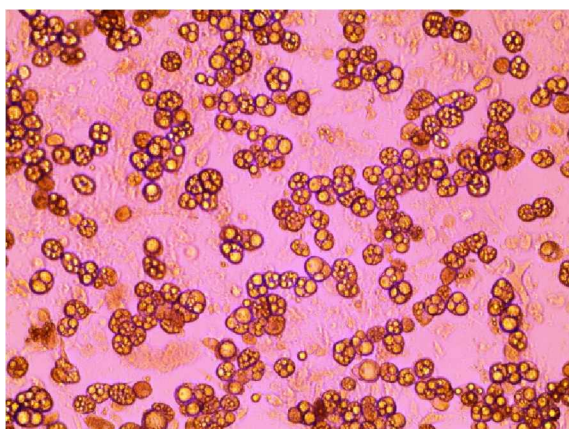
Surprising morphologies were seen in population 7 on day 26; rarely some healthy cells were seen. Sudden inflation of some lipid droplets was also observed. Along with this, tiniest lipid droplets were also seen in this population. The reason of these anomalies in cell size is an interesting thing to address. Some cells appeared to have developed thin blackish covering like cyst covering around them. Cells in population 8 showed less number of cells with higher scattering, size and shape of cells were highly abnormal and distorted when compared to the normal cells. Dominance of pre-adipocytes, through abnormal cells could be seen suggesting that most cells failed to survive at this point of cell culture. It is possible to see some cell growth after another 48 hours because cells have been provided with fresh medium treatment.



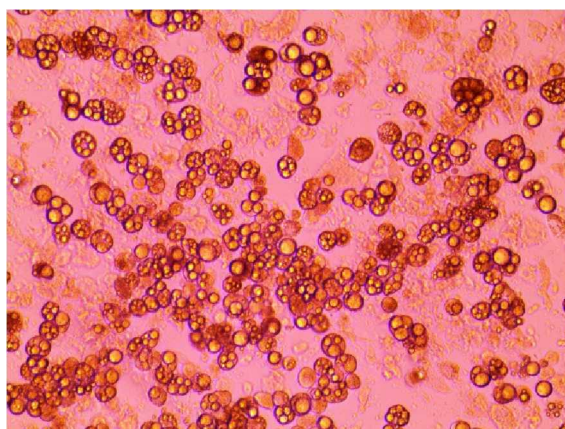
Population 1: Control



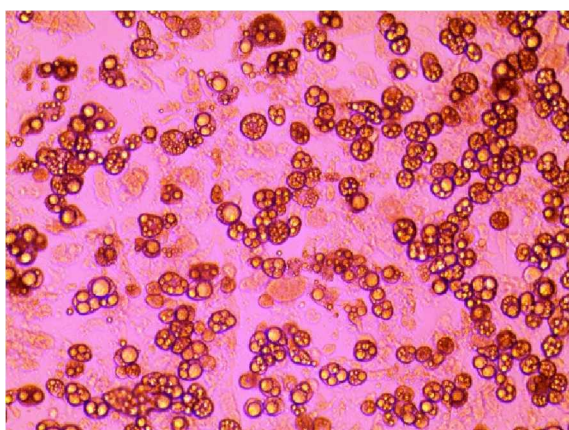
Population 2: MeHg



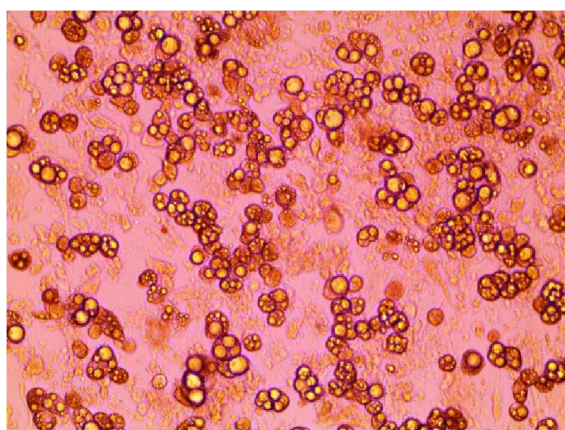
Population 3: MeHg + 3.14 μM TF-3



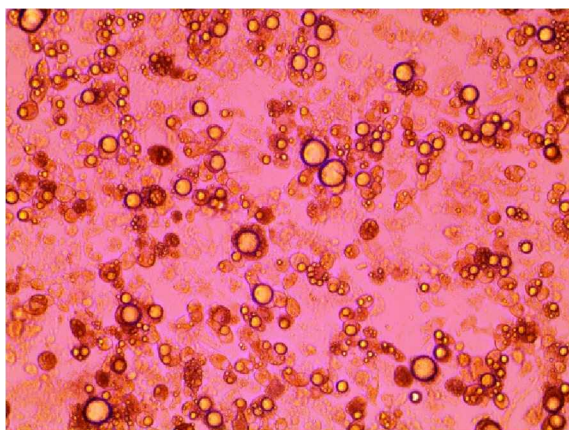
Population 4: MeHg + 6.25 μM TF-3



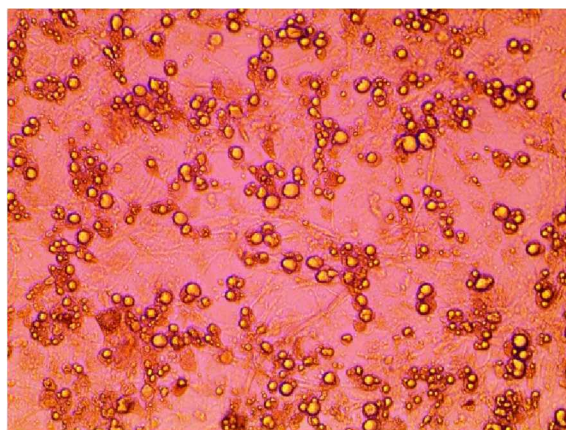
Population 5: MeHg + 12.5 μM TF-3



Population 6: MeHg + 25 μM TF-3



Population 7: MeHg + 50 μ M TF-3



Population 8: MeHg + 100 μ M TF-3

Figure 3.1g: Morphology changes caused due to different treatments to mature adipocytes on Day 26.

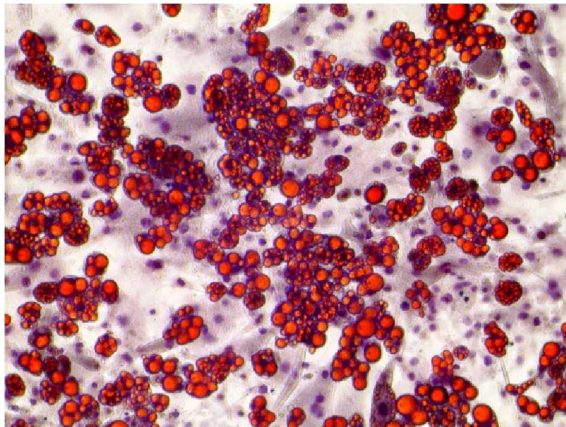
3.1.6 Morphological changes in 3T3-L1 adipocytes on Day 28 upon exposure to MeHg and TF-3 using Oil Red O.

Figure 3.1h shows set of images of oil red o stained cell populations on day 28. Lipid staining helps to differentiate between differentiated and non differentiated cells. Lipid droplets are indicative of successful differentiation and will turn red in color, whereas nuclei will turn blue in color. Cells in population 1 clearly shows that red color is dominating suggesting successful maintenance of differentiated of 3T3-L1 adipocytes even at day 28 showing mature cells with spherically distinct lipid droplets. However, in population 2 red stains can minimally be seen suggesting smaller number of adipocytes survival.

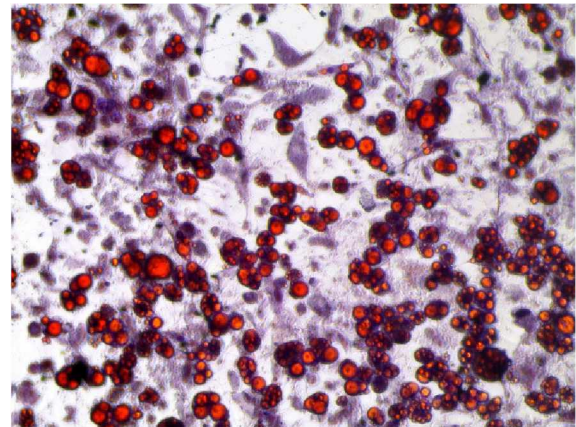
In population 3, lesser red stained cells can be seen when compared to population 1 but is clearly better than population 2 suggesting positive effects from TF-3. Higher number of red stained cells among all other treated groups can be seen in population 4 suggesting TF-3 helped cells to maintain their standard morphology even after exposure to MeHg. Cells in

population 5 are similar to population 3; however cell number is slightly less. As compared to the control cells population, a higher percentage of surface area is devoid of adipocytes.

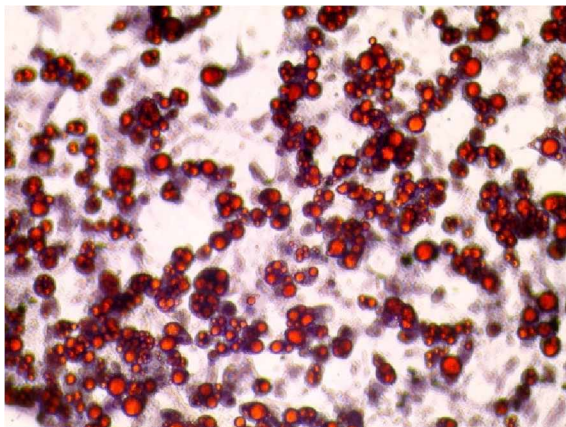
Population 6 shows presence of cells even at this high concentration of TF-3 along with MeHg exposed cells; however few cells are present which are highly dispersed. In population 7, fewest cells are present along with the tiniest lipid droplets. The cell number is comparatively very small to control group. A scattered mesh of pre-adipocytes can also be seen which is surprising. Low numbers of red stained cells were seen but were more than population 2 and 7; shape and size of lipid droplets were similar to population 7. Almost no cell clumping could be seen because of lesser number of survived cells.



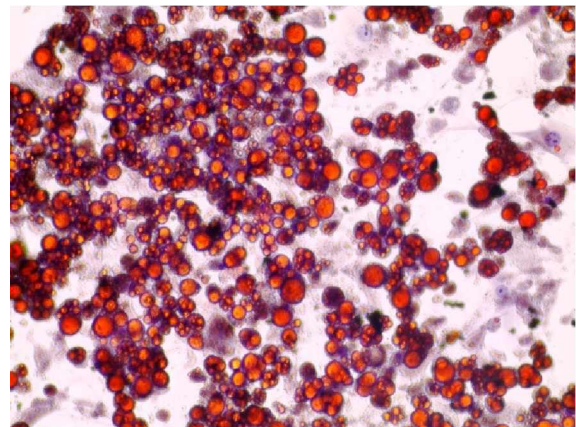
Population 1: Control



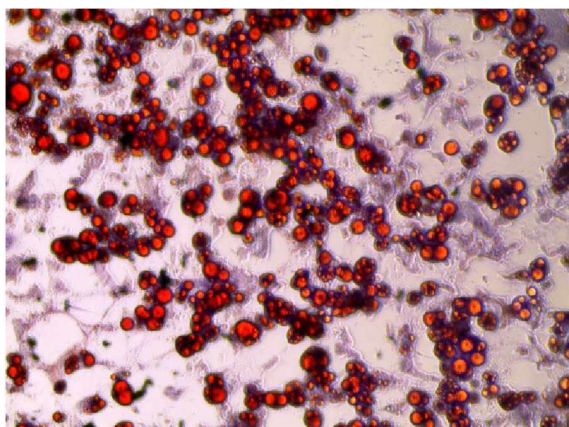
Population 2: MeHg



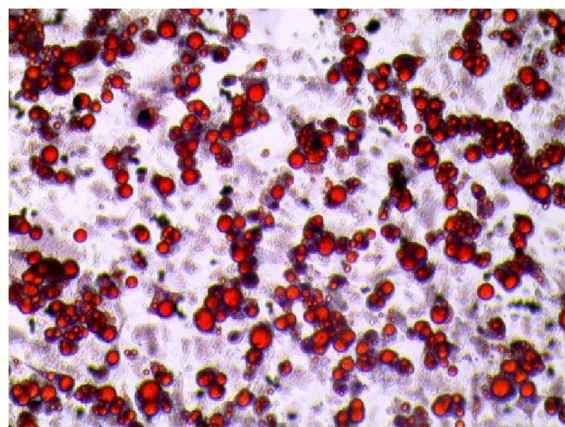
Population 3: MeHg + 3.14 μ M TF-3



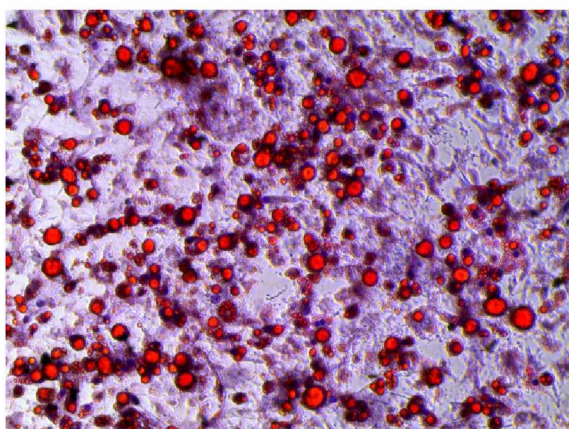
Population 4: MeHg + 6.25 μ M TF-3



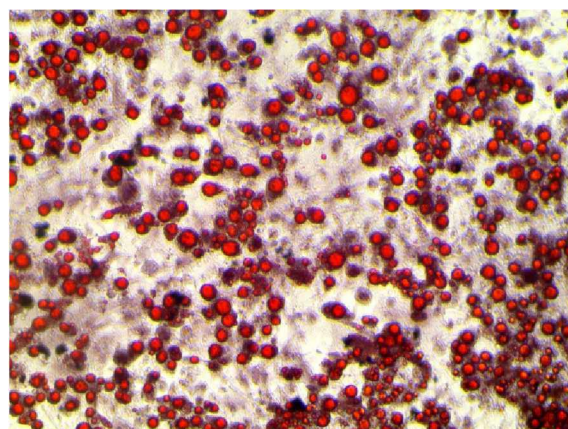
Population 5: MeHg + 12.5 μ M TF-3



Population 6: MeHg + 25 μ M TF-3



Population 7: MeHg + 50 μ M TF-3



Population 8: MeHg + 100 μ M TF-3

Figure 3.1h: Morphology changes caused due to different treatments to mature adipocytes on Day 28 using lipid staining.

3.2 Effects of MeHg and TF-3 on the secretion patterns of adiponectin

3.2.1 Basal levels of adiponectin secreted from control population of 3T3-L1 cells

Quantification of adiponectin levels at various points was conducted by using commercially available ELISA kits on the cell culture medium which contained the secreted protein of interest. For determining the basal levels of adiponectin secreted from non-differentiated and differentiated adipocytes, samples were collected from day 0 to day 28 of the culture period. Cells were grown in triplicates; three samples were collected from three different wells for each day every 48 hours over 28 days. A total of 45 samples were obtained for analyzing the secretions from days 0 - 28 , to monitor the secretion pattern of adiponectin at different growth (incubation) stages, such as growth, differentiation and maintenance (Figure 3.2a).

During the initial growth phase, the secretion levels of adiponectin were almost negligible. On day 0 the adiponectin concentration was 0.96 ± 0.70 ng/mL which increased to 19.4 ± 0.80 ng/mL on day 6. A significant increase in adiponectin secretion was seen from day 6 onwards when the differentiation process of pre-adipocytes started taking place. On day 12 when cells had started to incubate in maintenance medium, the secretion dropped to 39.3 ± 1.6 ng/mL as compared to day 10 where the level was 47.2 ± 0.4 ng/mL. From day 12 onwards, the secretion levels were decreased a little as a small downward secretion pattern developed. It appears to have formed a plateau pattern with no significant increase or decrease in secretion. On day 20, the level was 38.8 ± 0.7 ng/mL. A gradual drop is expected as cells were aging. The level of adiponectin detected was 33.5 ± 0.9 ng/mL on day 28.

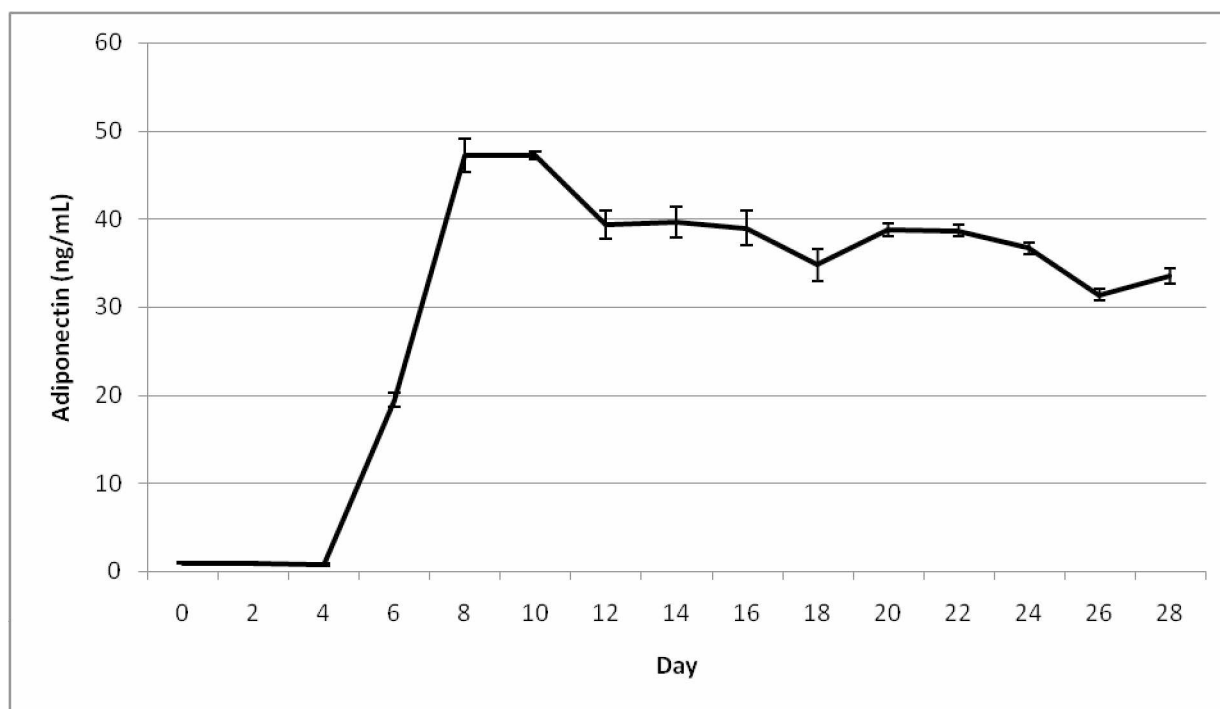


Figure 3.2a Basal adiponectin levels secreted from 3T3-L1 cells (Day 0 to Day 28)

3.2.2 Effect of MeHg exposure on adiponectin secretion from 3T3-L1 cells (Day 18 - Day 28).

Cell culture medium from day 18 to day 28 from three different wells were collected and stored. The cells' maintenance medium during days 18 - 28 were used to compare the adiponectin secretion between MeHg exposed and control cells. The concentration levels were calculated and the collective mean was obtained from days 18 - 28 to determine the statistical significance of the data presented. Mann-Whitney U test was performed on values obtained from day 18 - day 28. As the cells were grown in triplicates, the number of samples was fifteen for each population (n=15). The mean concentration of adiponectin secretion in control cells (population 1) from day 18 - day 28 was 35.8 ± 3 ng/mL. However, MeHg exposure on the mature cells

resulted in significance increase in adiponectin levels. The mean adiponectin concentration from day 18 - day 28 was 54.1 ± 4.0 ng/mL (Figure 3.2b).

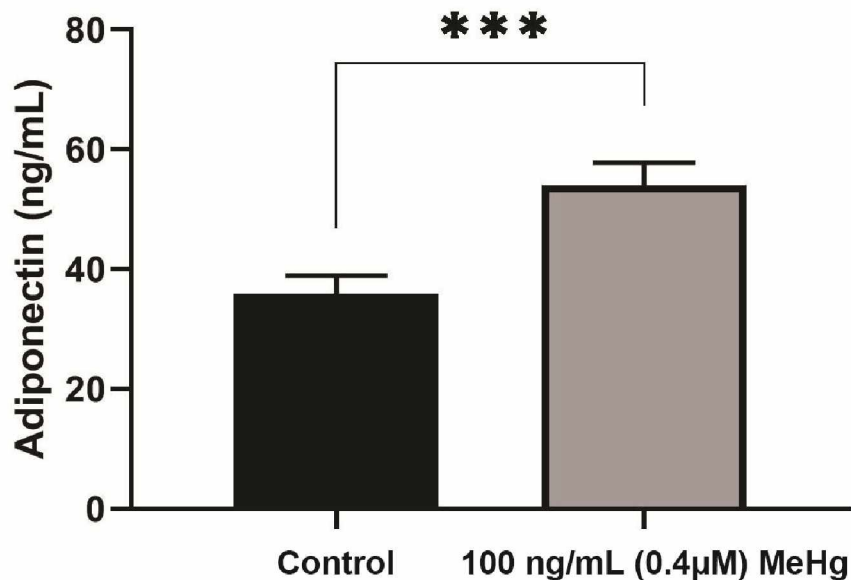


Figure 3.2b: Adiponectin secretion from control cells (population 1) and MeHg exposed cells (population 2) from day 18 - day 28; p-value was less than 0.0001.

3.2.3 Effect of MeHg+3.14 μ M TF-3 exposure on adiponectin secretion from 3T3-L1 cells (Day 18 - Day 28).

Cell culture media from day 18 to day 28 from three different wells of population 3 were used to determine the difference between two populations (1 and 3). A total of 15 samples were used to analyze the adiponectin secretion levels between control and MeHg exposed + TF-3 treated cells. Student's t - test was performed on data collected to determine the statistical significance. The mean concentration of adiponectin secretion in control cells (population 1) from day 18 - day 28 was 35.8 ± 3.1 ng/mL MeHg + 3.14 μ M TF-3 exposure on the mature cells showed significance increase in adiponectin levels (Figure 3.2c). It was expected that tea addition would

counteract the MeHg effect and restore adiponectin levels close to that of control cells. 3.14 μ M TF-3 increased adiponectin secretion levels even more. The mean adiponectin concentration from day 20 - day 28 in population 3 was 56.9 ± 6.0 ng/mL (Figure 3.2c).

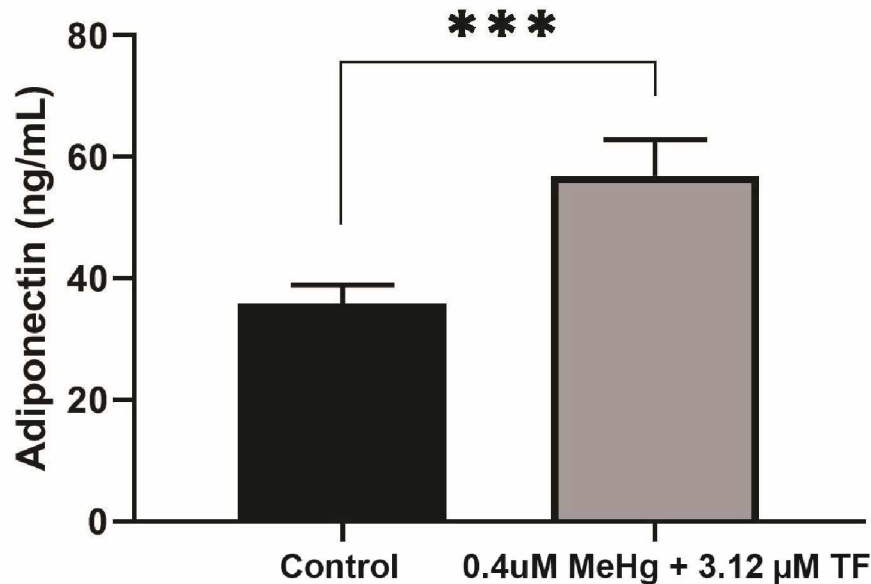


Figure 3.2c: Adiponectin secretion from control cells (population 1) and MeHg + 3.14 μ M TF-3 exposed cells (population 3) from day 18 - day 28; p-value was less than 0.0001.

3.2.4 Effect of MeHg+6.25 μ M TF-3 exposure on adiponectin secretion from 3T3-L1 cells (Day 18 - Day 28).

Collected cell culture media from day 18 - day 28 were analyzed to determine the difference between control and treated cell populations. The populations were grown in triplicates and the collective number of samples was fifteen (n=15) for population 4. Student's t-test was performed on data collected to determine the statistical significance between population 1 (control cells) and population 4 (Figure 3.2d). Although, treatment of MeHg exposed cells with 6.25 μ M TF-3 did counteract the MeHg secretion effect, it was lower than population 2 because the

concentration of adiponectin secretion in population 2 (MeHg exposed) was 54.1 ± 4 ng/mL but in population 4 (MeHg + 6.25 μ M) it was 50.6 ± 8 ng/ml. The reported standard deviation is greater in population 4. The reported mean concentration of adiponectin secretion in control cells (population 1) from day 18 - day 28 was 35.8 ± 3.1 ng/mL. The mean adiponectin concentration in population 4 (MeHg + 6.25 μ M TF-3) from day 18 - day 28 was 50.6 ± 8.0 ng/ml (Figure 3.2d).

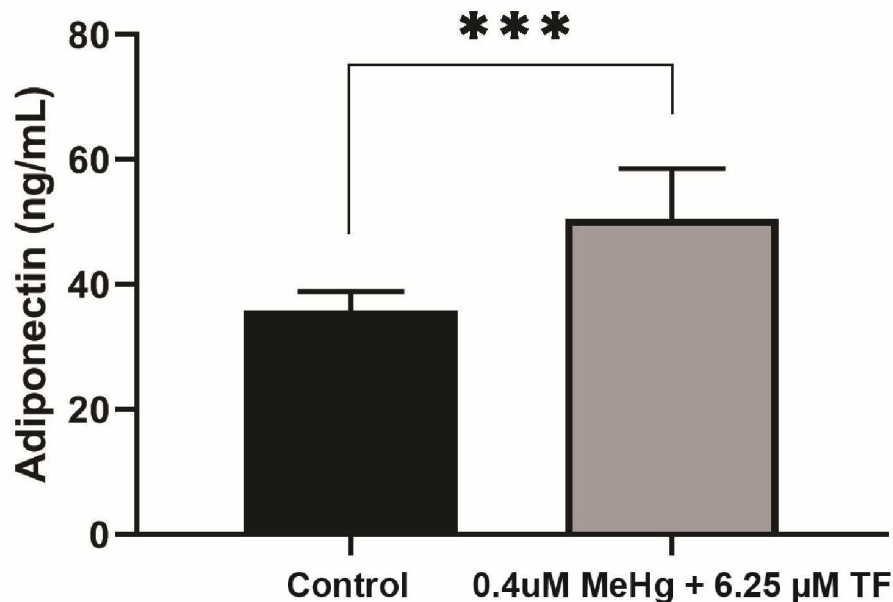


Figure 3.2d: Adiponectin secretion from control cells (population 1) and MeHg + 6.25 μ M TF-3 exposed cells (population 4) from day 18 - day 28; p-value was less than 0.0001.

3.2.5 Effect of MeHg + 12.5 μ M TF-3 exposure on adiponectin secretion from 3T3-L1 cells (Day 18 - Day 28).

For determining the statistical difference between populations 1 and 5, Student's t-test was performed on data obtained from the analysis of cell culture media collected and stored from day 18 to day 28 from population 5. The populations were grown in triplicates and the collective number of samples was fifteen (n=15) for population 5. The collective mean concentration of

adiponectin calculated in population 5 from day 18 - day 28 was 51.6 ± 4.2 ng/mL. The concentration of TF-3 was increased to $12.5 \mu\text{M}$ in this case, but it turned out to have a similar effect as seen in population 4 (Figure 3.2e). The mean concentration of adiponectin secretion in control cells (population 1) from day 18 - day 28 was 35.8 ± 3.1 ng/mL. The mean adiponectin concentration in population 5 (MeHg + $12.5 \mu\text{M}$ TF-3) from day 18 - day 28 was 51.6 ± 4.2 ng/mL (Figure 3.2e).

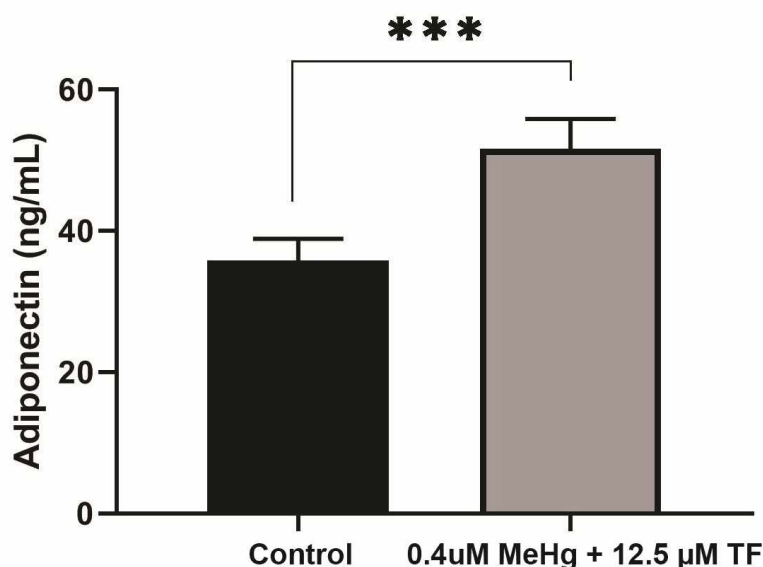


Figure 3.2e: Adiponectin secretion from control cells (population 1) and MeHg + $12.5 \mu\text{M}$ TF-3 exposed cells (population 5) from day 18- day 28; p-value was less than 0.0001.

3.2.6 Effect of MeHg + $25 \mu\text{M}$ TF-3 exposure on adiponectin secretion from 3T3-L1 cells (Day 18-Day 28).

The collective mean concentration of adiponectin calculated in population 6 (MeHg + $25 \mu\text{M}$) from day 18 – day 28 was 41.4 ± 5.0 ng/mL. This concentration was closest to the adiponectin secretion level found in control cells population which was 35.8 ± 3.1 ng/mL. MeHg exposure, which caused a significant increase in adiponectin secretion levels (Figure 3.2b), was partly

restored by treatment of cells with 25 μ M TF-3 (Figure 3.2f). Student's t-test was performed on data obtained from the analysis of cell culture media collected and stored from day 18 to day 28 from populations 1 and 6. The mean concentration of adiponectin secretion in control cells (population 1) from day 18 - day 28 was 35.8 ± 3.1 ng/mL. The mean adiponectin concentration in population 6 (MeHg + 25 μ M TF-3) from day 20-day 28 was 41.4 ± 5.0 ng/mL.

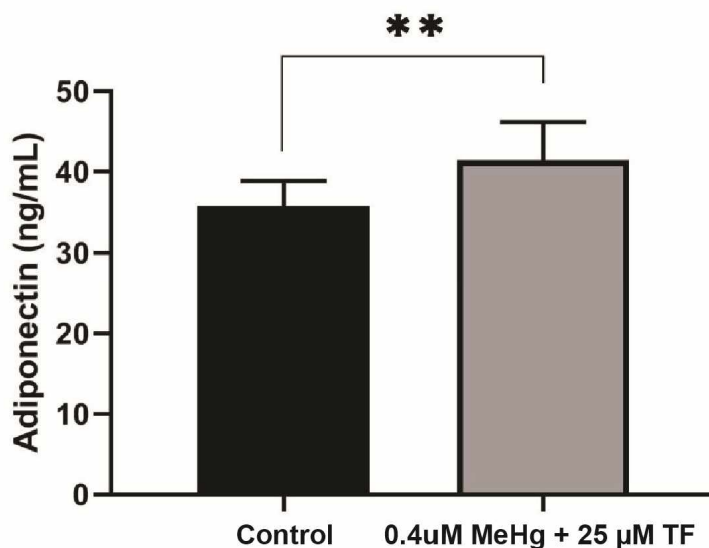


Figure 3.2f: Adiponectin secretion from control cells (population 1) and MeHg + 25 μ M TF-3 exposed cells (population 6) from day 18 - day 28; p-value was 0.0006.

3.2.7 Effect of MeHg + 50 μ M TF-3 exposure on adiponectin secretion from 3T3-L1 cells (Day 18-Day 28).

In this population, TF-3 concentration was 50 μ M which was the second highest concentration used in this study. Surprising results were obtained from this population as the adiponectin concentration was 13.4 ± 15 ng/mL which was lower than the control adiponectin level (35.8 ± 3.0 ng/mL). The reported standard deviation is a larger number indicating uncertainty in the calculated value. Mann-Whitney U test was performed on data collected to determine the

statistical significance. Bonferroni correction showed that the p-value in this case was 0.0023; and alpha-level after Bonferroni correction was 0.00625 instead of 0.05; therefore this data set was found to be significantly lower (Figure 3.2g).

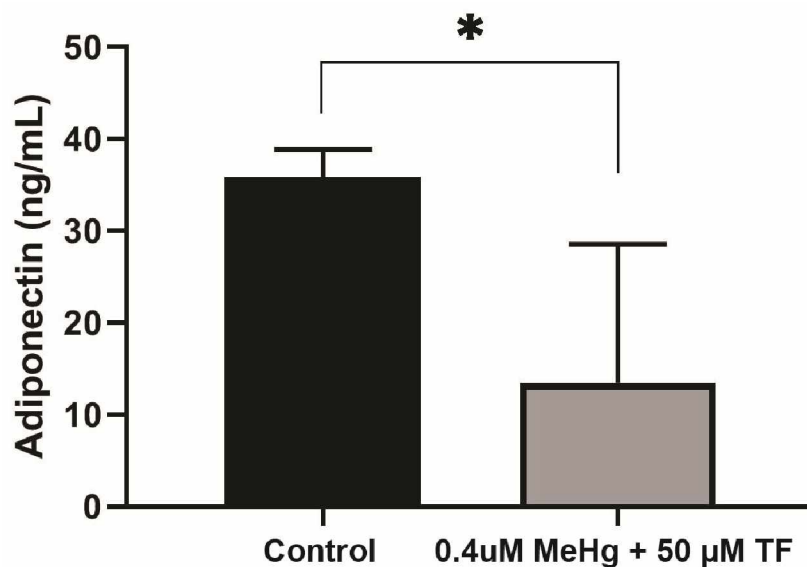


Figure 3.2g: Adiponectin secretion from control cells (population 1) and MeHg + 50 μ M TF-3 exposed cells (population 7) from day 18 - day 28; p-value was 0.0023.

3.2.8 Effect of MeHg + 100 μ M TF-3 exposure on adiponectin secretion from 3T3-L1 cells (Day 18-Day 28).

To determine the effect of highest concentration of TF-3 (100 μ M) used in this study on adiponectin secretions, samples were collected and stored from day 18 to day 28. Mann-Whitney U test was performed on data collected to determine the statistical significance. Since adiponectin concentration in population 7 was smaller as compared to population 1, it was expected that adiponectin concentration in this population 8 will be even smaller as the TF-3 levels was double in quantity as compared to population 7. The mean concentration of adiponectin secretion in control cells (population 1) from day 18 - day 28 was 35.80 ± 3.0 ng/mL.

The mean adiponectin concentration in population 8 (MeHg + 100 μ M TF-3) from day 18 - day 28 was 8.9 ± 9.0 ng/mL (Figure 3.2h).

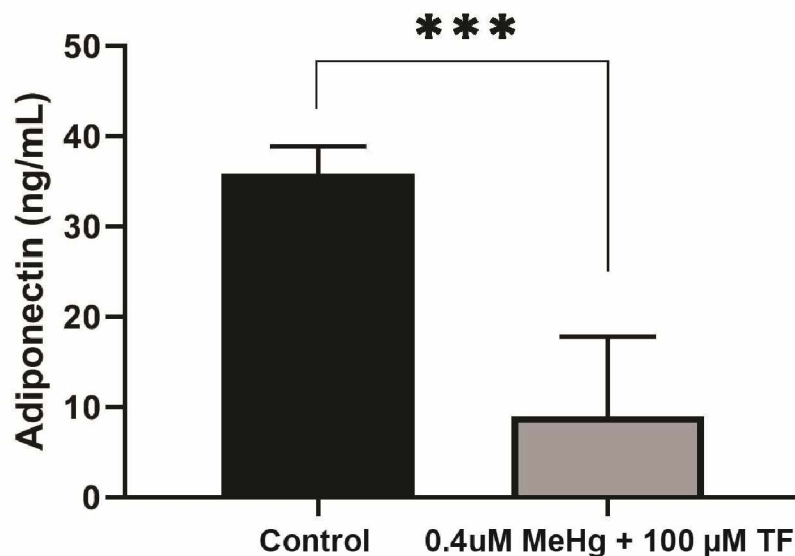


Figure 3.2h: Adiponectin secretion from control cells (population 1) and MeHg + 100 μ M TF-3 exposed cells (population 8) from day 18 - day 28; p-value was less than 0.0001.

3.2.9 Overall analysis of adiponectin concentrations from population 1 to population 8

To determine the overall statistical significance of data obtained from various populations, Kruskal Wallis analysis of variance was performed. The reported p-value was less than 0.0001 and the entire study was found to be extremely significantly different. Adiponectin concentration in both concentration ends of treatment with TF-3 resulted in either higher value or lower values as compared to the control. Treatment of MeHg exposed cells with 25 μ M TF-3 turned out to be the most appropriate and efficient concentration. 25uM restored the adiponectin concentration closer to the control group. Other TF-3 concentrations such as 3.14, 6.25 and 12.5 μ M which comparatively increased secretion levels while 50 and 100 μ M TF-3 concentrations greatly decreased adiponectin levels.

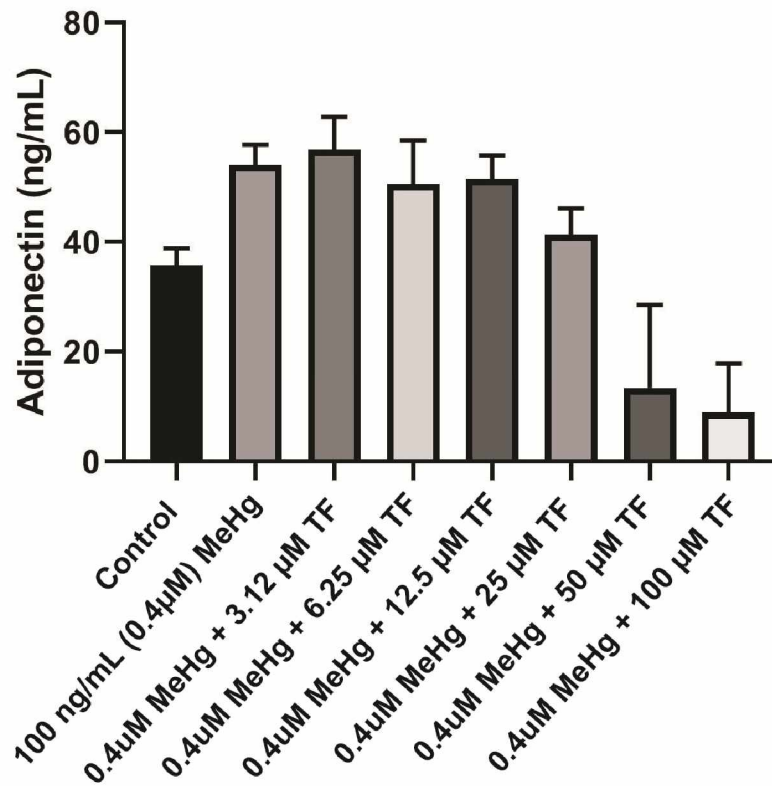


Figure 3.2i: Adiponectin secretion in all eight populations from day 18 - day 28. Overall statistically significant difference was determined using Kruskal-Wallis method and p-value was less than 0.0001.

3.3 Effects of MeHg and TF-3 on the secretion patterns of resistin

3.3.1 Basal levels of resistin secreted from control population of 3T3-L1 cells.

Quantification of resistin levels at various points was conducted by using commercially available ELISA kits on the cell culture medium which contained the secreted protein of interest. Cell culture media samples were collected from day 0 to day 28 of the culture period for determining the basal levels of resistin secreted from non-differentiated and differentiated adipocytes. Cells were grown as triplicates, three samples were collected from three different wells for each day at every 48 hours over 28 days (a total of 45 samples were obtained for analyzing the secretions from day 0 – day 28), to monitor the secretion pattern of resistin at different phases (incubation) stages such as growth, differentiation and maintenance (Figure 3.3a).

Figure 3.3a shows that during initial growth of pre-adipocytes there was an absence of resistin secretion. From day 4 onwards, which is when pre-adipocytes cells were growing in differentiation medium, were developing into spherical shaped adipocytes cells. On day 6, when cells were incubated in insulin medium, a prominent increase in resistin concentration of 11371.4 ± 119.0 pg/mL was observed. Furthermore on day 12, a drop in resistin concentration could be seen, but it increased in the next four days. A regular downward secretion pattern of resistin occurred from day 18 onwards when the concentration dropped down to 8498.06 ± 99.0 pg/mL on day 28.

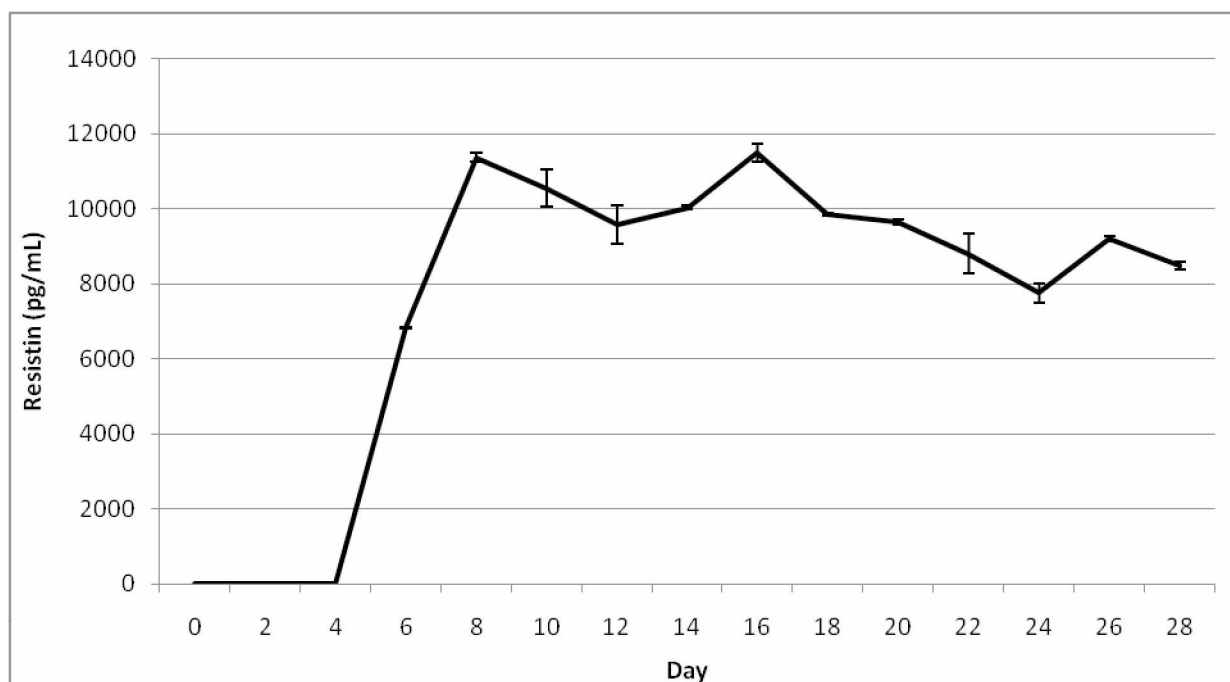


Figure 3.3a: Basal resistin levels secreted from 3T3-L1 cells (Day 0 to Day 28)

3.3.2 Effect of MeHg exposure on resistin secretion from 3T3-L1 cells (Day 18 - Day 28).

To determine the effect of MeHg exposure upon resistin concentration, cell culture media from both population 1 (control) and population 2 (MeHg exposed) were collected and stored.

Concentrations of resistin under different treatments were quantified using ELISA. Mann-Whitney U test was performed on values obtained from day 18 - day 28. As the cells were grown in triplicates, the number of samples was fifteen for each population (n=15). The mean concentration of resistin secretion in control cells (population 1) from day 18 - day 28 was calculated as 8781.4 ± 705.0 pg/mL.

MeHg exposure on the mature cells caused a significance increase in resistin levels during the exposure study (Figure 3.3c). The mean resistin concentration from day 18 - day 28 was calculated as 9717.3 ± 3914.0 pg/mL. During the first six days (day 18 - day 24) of treatment

MeHg significantly increased resistin concentration, but, during the last four days (day 24 - day 28) the change in resistin secretion level declined and was not significant as the values were decreased. Lower values for resistin concentration during last four days hence increased the value of the standard deviation, since the drop there was a sudden drop which may be related to an increase in cell death.

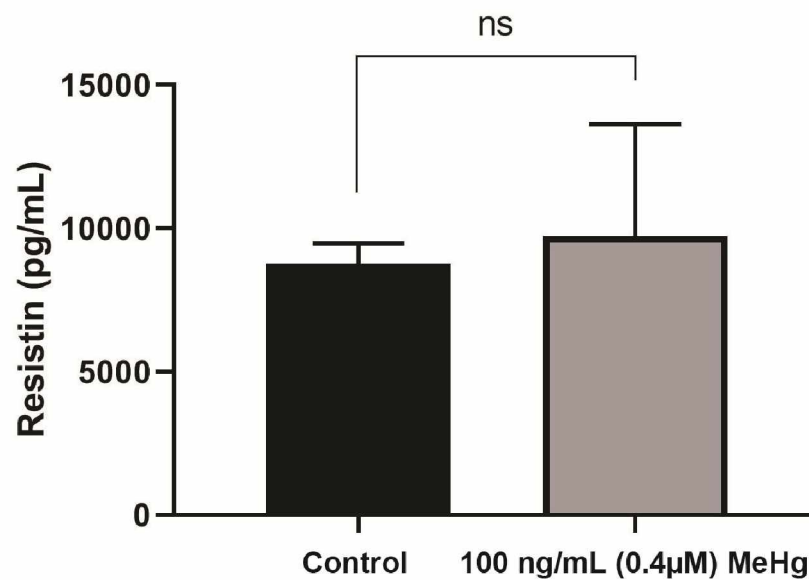


Figure 3.3b: Resistin secretion from control cells (population 1) and MeHg exposed cells (population 2) from day 18 - day 28; p-value was 0.3453.

3.3.3 Effect of MeHg + 3.14 μM TF-3 exposure on resistin secretion from 3T3-L1 cells (Day 18 - Day 28).

Mann-Whitney U test was performed on data collected to determine the statistical significance. There was no statistical difference between data obtained from population 1 and population 3 with MeHg and 3.14 μM. A greater value of standard deviation was obtained and low values for resistin concentration were observed during the last four days of the study. The previous results showed 3.14 μM TF-3 increased adiponectin levels in MeHg exposed cells. The mean

concentration of resistin secretion in control cells (population 1) from day 18 - day 28 was 8781.4 ± 705.0 pg/mL. The mean resistin concentration in population 3 (MeHg + $3.14 \mu\text{M}$ TF-3) from day 18 - day 28 was calculated as 8841.5 ± 5349.0 pg/mL (Figure 3.3c).

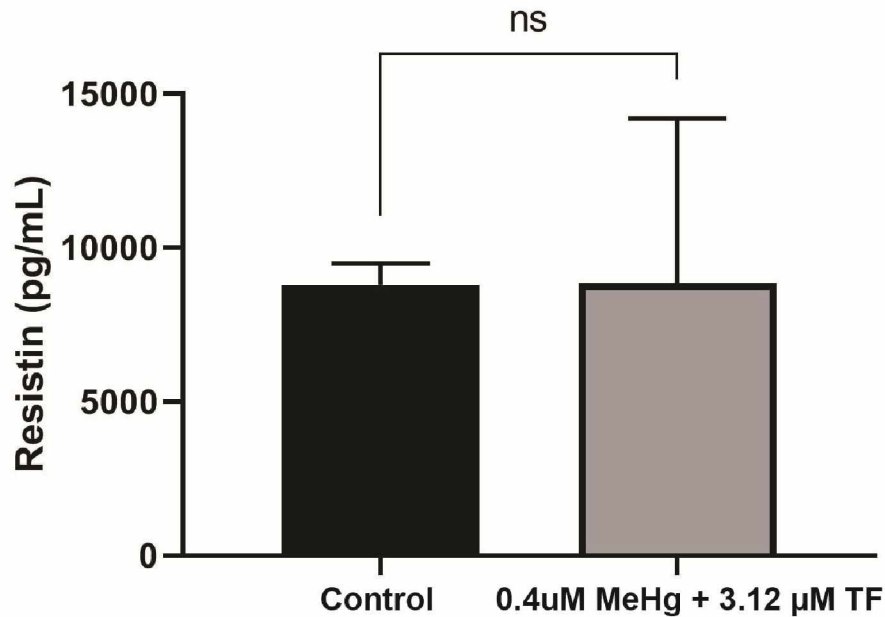


Figure 3.3c: Resistin secretion from control cells (population 1) and MeHg + $3.14 \mu\text{M}$ TF-3 exposed cells (population 3) from day 18 - day 28; p-value was 0.4864.

3.3.4 Effect of MeHg + $6.25 \mu\text{M}$ TF-3 exposure on resistin secretion from 3T3-L1 cells (Day 18 - Day 28).

Since, $3.14 \mu\text{M}$ TF-3 already had restored the resistin levels close to the control cells, it was expected that this higher concentration of TF-3 would further decrease resistin levels. It turned out that it did decrease the resistin concentration even more. The values from last four day continued getting lower and the standard deviation increased. Mann-Whitney U test was

performed on data collected to determine the statistical significance with $n=15$. Data obtained was not significantly different due to higher p-value. The mean concentration of resistin secretion in control cells (population 1) from day 18 - day 28 was calculated as 8781.4 ± 705.0 pg/mL. The mean resistin concentration in population 4 (MeHg + $6.25 \mu\text{M}$ TF-3) from day 18 - day 28 was calculated as 7616.0 ± 4489.0 pg/mL (Figure 3.3d). TF-3 was reducing the expression of resistin counteracting some of the effects of MeHg.

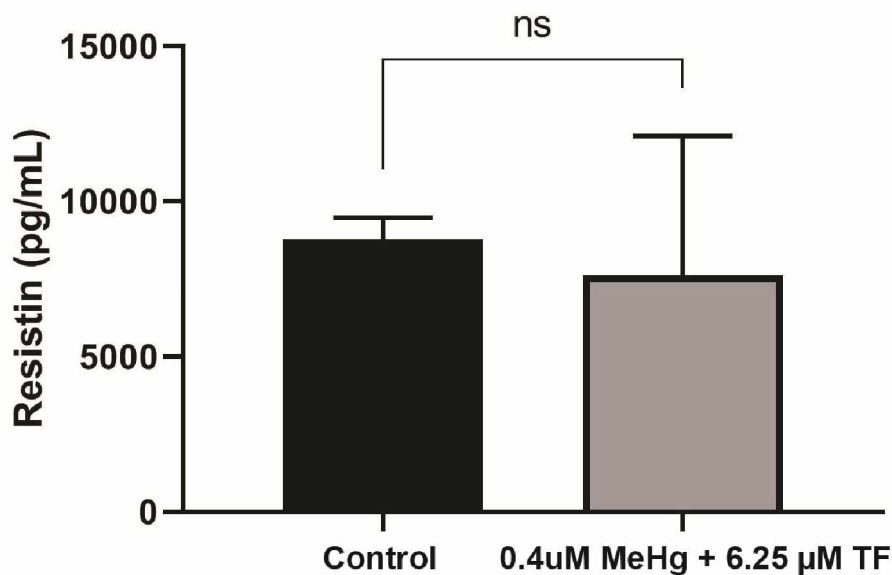


Figure 3.3d: Resistin secretion from control cells (population 1) and MeHg + $6.25 \mu\text{M}$ TF-3 exposed cells (population 4) from day 18 - day 28; p-value was 0.5125.

3.3.5 Effect of MeHg + $12.5 \mu\text{M}$ TF-3 exposure on resistin secretion from 3T3-L1 cells (Day 18 - Day 28).

Mann-Whitney U test was performed on data collected to determine the statistical significance between population 1 (control cells) and population 5 (MeHg + $12.5 \mu\text{M}$ TF-3). Values from populations 3 and 4 were not significantly different. The resistin concentration in population 3, suggested a positive aspect of treatment with TF-3. When TF-3 concentration was increased to

12.5 μM (population 5), resistin concentrations decreased even more. The mean concentration of resistin secretion in control cells (population 1) from day 18 - day 28 was 8781.4 ± 705.0 pg/mL. The mean resistin concentration in population 5 (MeHg + 12.5 μM TF-3) from day 18 - day 28 was 5964.6 ± 4387.0 pg/mL (Figure 3.3e).

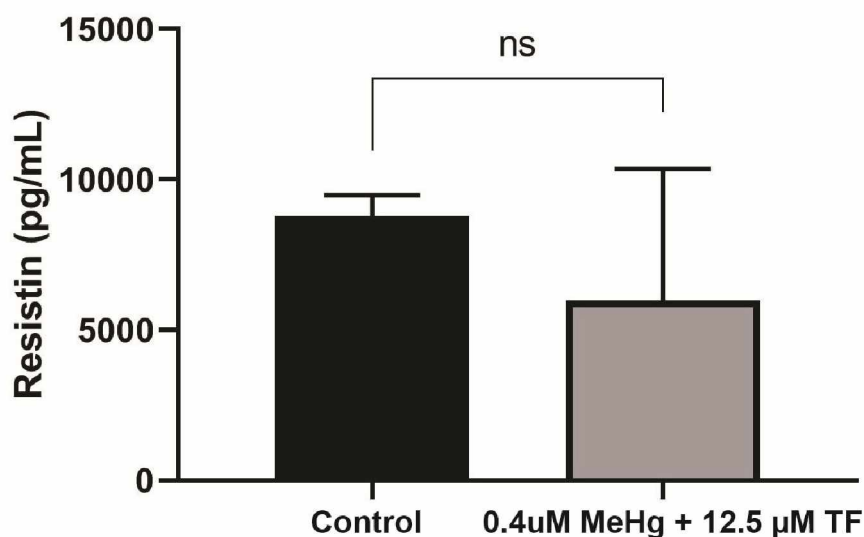


Figure 3.3e: Resistin secretion from control cells (population 1) and MeHg + 12.5 μM TF-3 exposed cells (population 5) from day 18 - day 28; p-value was 0.3669.

3.3.6 Effect of MeHg + 25 μM TF-3 exposure on resistin secretion from 3T3-L1 cells (Day 18 - Day 28).

Although data was not statistical significant for population 6, it was expected that TF-3 is going to decrease resistin concentration further. The collective mean concentration of resistin calculated in population 6 from day 18 – day 28 was 1956.2 ± 2184.0 pg/mL. The mean concentration of resistin secretion in control cells (population 1) from day 18 - day 28 was 8781.4 ± 705.0 pg/mL. The mean resistin concentration in population 6 (MeHg + 25 μM TF-3)

from day 18 - day 28 was calculated as 1956.2 ± 2183.0 pg/mL (Figure 3.3f). Population 6 was significantly lower than control population 1.

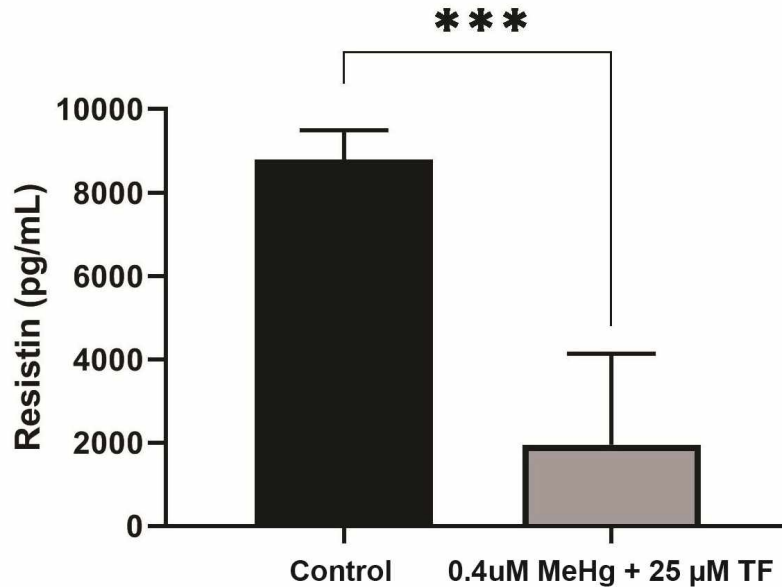


Figure 3.3f: Resistin secretion from control cells (population 1) and MeHg + 25 µM TF-3 exposed cells (population 6) from day 18 - day 28, p-value was less than 0.0001.

3.3.7 Effect of MeHg + 50 µM and MeHg + 100 µM TF-3 exposure on resistin secretion from 3T3-L1 cells (Day 18 - Day 28).

Mann-Whitney U test was performed on the data obtained from the experimental calculations of populations 1 and 7. Statistical significance was seen from population 6 onwards. TF-3 seemed to only decrease the resistin concentration. The mean concentration of resistin secretion in control cells (population 1) from day 18 - day 28 was 8781.4 ± 705.0 pg/mL. The mean resistin concentration in population 7 (MeHg + 50 µM TF-3) from day 20 - day 28 was 1255.0 ± 1899.0 pg/mL (Figure 3.3g).

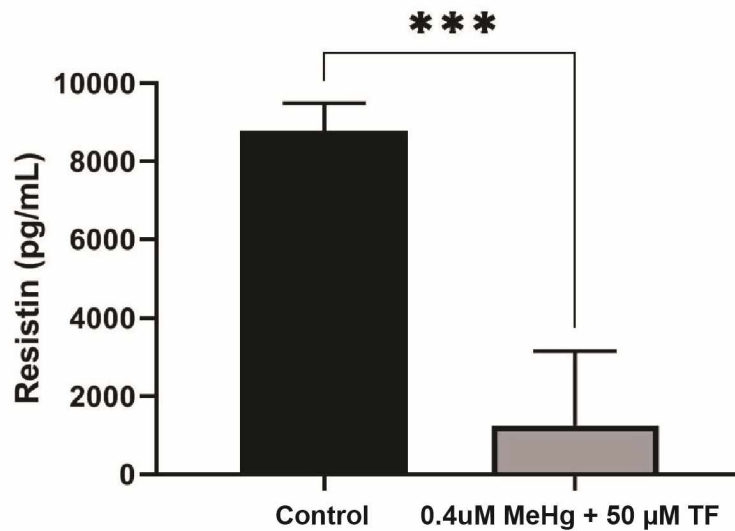


Figure 3.3g: Resistin secretion from control cells (population 1) and MeHg + 50 µM TF-3 exposed cells (population 7) from day 18 - day 28; p-value was less than 0.0001.

The effects of 50 and 100 µM TF-3 were very similar. The mean concentration of resistin secretion in control cells (population 1) from day 18 - day 28 was 8781.4 ± 705.0 pg/mL. The mean resistin concentration in population 8 (MeHg + 100 µM TF-3) from day 18 - day 28 was 1224.4 ± 1882.0 pg/mL (Figure 3.3h).

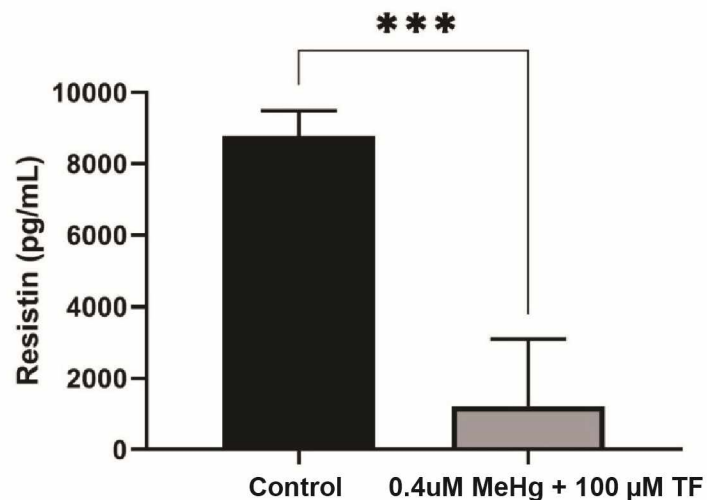


Figure 3.3h: Resistin secretion from control cells (population 1) and MeHg + 100 µM TF-3 exposed cells (population 8) from day 18 - day 28; p-value was less than 0.0001.

3.3.8 Overall analysis of resistin concentrations from population 1 to population 8

The entire study was found to be significantly different having different medians using Kruskal Wallis test. However, when Mann-Whitney test on single pair of populations was used, some populations were not statistically significant compared to the control group. Values from day 26 and day 28 were far lower. Data from day 20 to day 26 in all populations were extremely statistically significant.

However, the overall difference was found to be significant. TF-3 reduced the increased resistin levels in population 3 onwards which is a positive aspect of its effect on MeHg exposed cells. Population 2 appears to have the highest concentration of resistin compared to other groups. Population 3 has similar level of resistin as that of population 1. It is quite evident that from population 4 onwards a decreasing trend can be seen, suggesting TF-3 effectiveness in combating effects of MeHg. However, populations 6, 7 and 8 secreted much smaller amounts of resistin when compared to population 1 (Figure 3.3i).

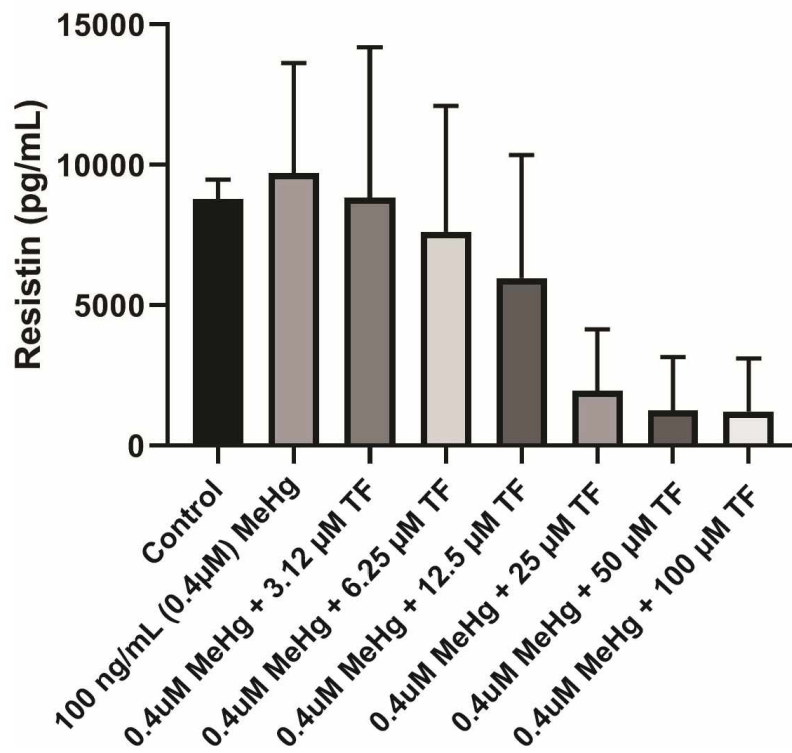


Figure 3.3i: Resistin secretion in all eight populations from day 18 - day 28. Overall statistically significant difference was determined using Kruskal-Wallis method and p-value was less than 0.0001

3.4 Effects of MeHg and TF-3 on 4 - Hydroxynonenal (4-HNE) secreted from 3T3-L1 adipocytes

3.4.1 Basal 4-HNE levels secreted from 3T3-L1 adipocytes.

MeHg increased ROS levels leading to an increase in oxidative stress. Levels of 4-HNE were studied to determine whether TF-3 could restore secretion level close to control. Cell culture media from control cells was collected. Since samples were collected thrice from three different wells of the same population, a total of 45 samples were collected over the period of 28 days. Using a 4-HNE ELISA, the 4-HNE concentrations at each day were measured. Figure 3.4a shows the basal secretion pattern of 4-HNE from 3T3-L1 cells in control cells over the course of 28 days.

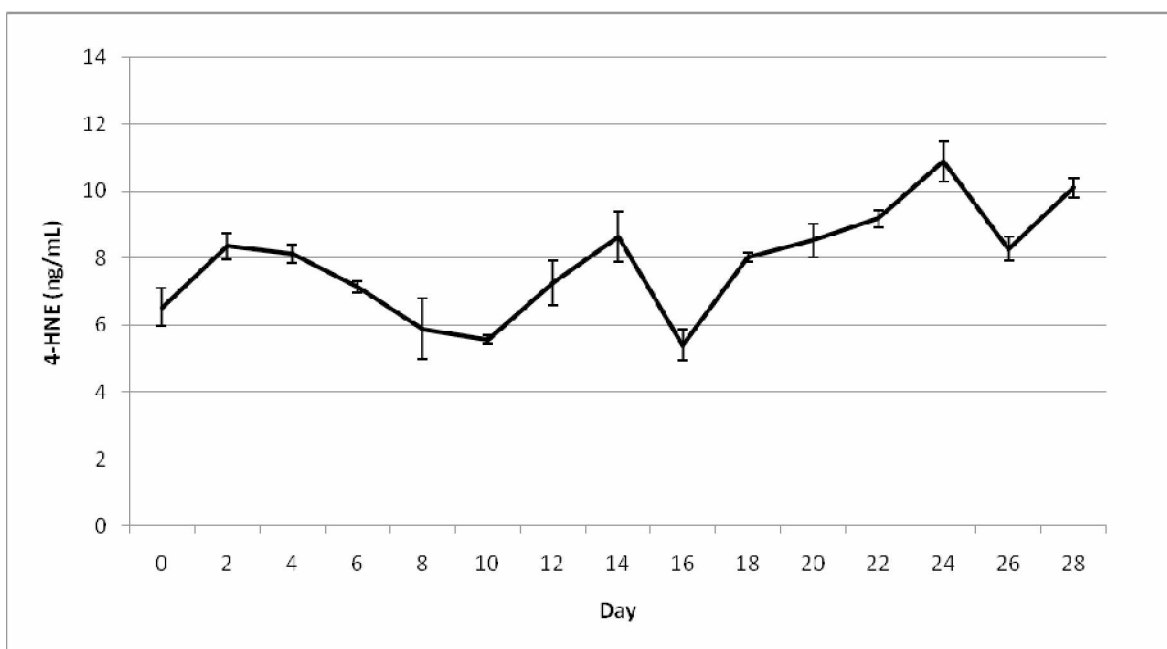


Figure 3.4a: Basal 4-HNE levels secreted from 3T3-L1 cells (Day 0 to Day 28)

In Figure 3.4a, it can be seen that 4-HNE secretion started from day 0 of growing pre-adipocytes. Adiponectin and resistin showed a several day delay (Figures 3.2a and 3.3a). The concentration of 4-HNE ranged from 6.5 ± 0.6 ng/mL on day 0 to 10.1 ± 0.3 ng/mL on day 28. A 20 to 40% variation in 4-HNE indicates random increasing and decreasing levels of ROS formation throughout the differentiation and maturation processes in 3T3-L1 cells (figure 3.4a).

3.4.2 Effects of MeHg and MeHg + TF-3 on the secretion of 4-HNE level

Overall statistically significant difference between different treatment groups was determined using Kruskal-Wallis method and p-value was less than 0.0001.

To determine the individual statistical significance between population 1 and 2 and other treated groups with respect to control group either Mann Whitney or Student's T test were performed.

The mean value of 4-HNE levels in population 1 is 4.4 ± 1.1 ng/mL for the last ten days. MeHg did increase the concentration of 4-HNE up to 11.90 ± 2.1 ng/mL. Mann Whitney U test was applied between populations 1 and 2 and it was found that the data is significantly different having a p-value of 0.0012 (Figure 3.4b).

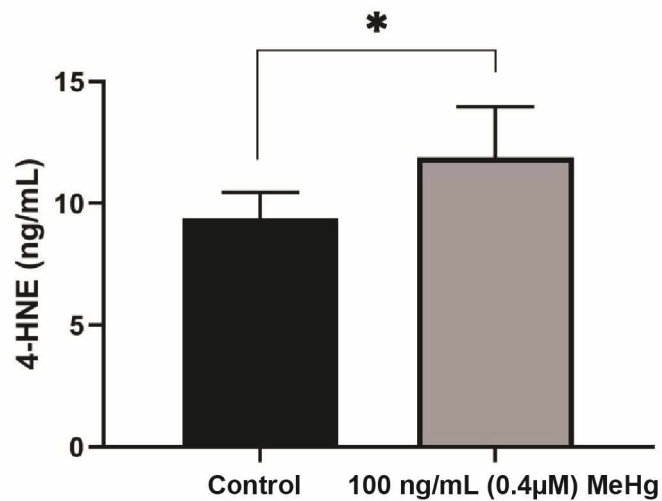


Figure 3.4b: 4-HNE secretion from control cells (population 1) and MeHg exposed cells (population 2) from day 18 - day 28; p-value was 0.0012.

On treatment with 3.14 μM TF-3, the increase in 4-HNE concentration due to MeHg exposure was restored to 2.2 ± 2.2 ng/mL which is close to the control population level. The Mann-Whitney test showed the data to be non significant having a p-value of 0.1370 (Figure 3.4c).

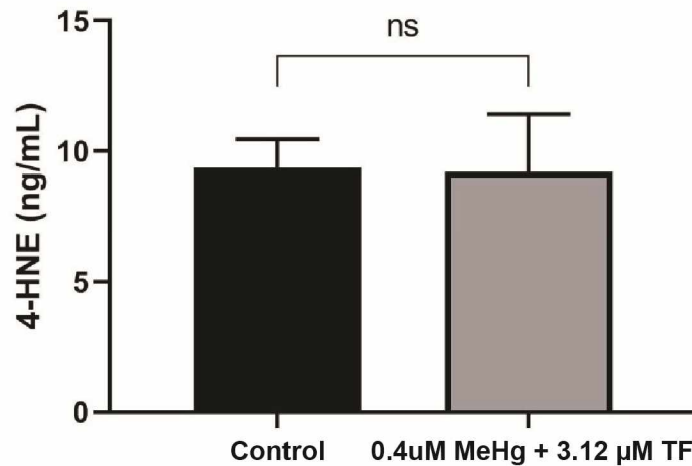


Figure 3.4c: 4-HNE secretion from control cells (population 1) and MeHg + 3.14 μM TF-3 exposed cells (population 3) from day 18 - day 28; p-value was 0.1370.

Population 4 shows levels of 4-HNE continuing to decrease and less than population 2. It is slightly higher than control levels, having a concentration of 7.2 ± 2.0 ng/mL. Mann-Whitney test comparing control and population 4 showed a statistically significant difference with a p-value of 0.0006 (Figure 3.4d).

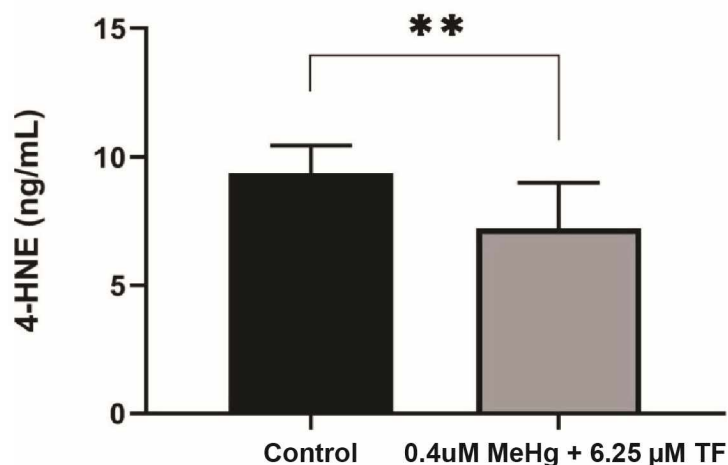


Figure 3.4d: 4-HNE secretion from control cells (population 1) and MeHg + 6.25 μM TF-3 exposed cell (population 4) from day 18 - day 28; p-value was 0.0006.

Surprisingly treatment of MeHg exposed cells with 12.5 and 25 μM drastically increased 4-HNE levels seen in populations 5 and 6. The mean of 4-HNE in populations 5 and 6 are 23.41 ± 13.38 ng/mL and 27.44 ± 5.43 ng/mL respectively. Mann-Whitney test between populations 1 and 5 suggested the compared data to be non significant with the reported p-value of 0.082 (Figure 3.4e). Student's T-test between population 1 and population 6 indicated data compared to be significantly different having a p-value < 0.0001 (Figure 3.4f).

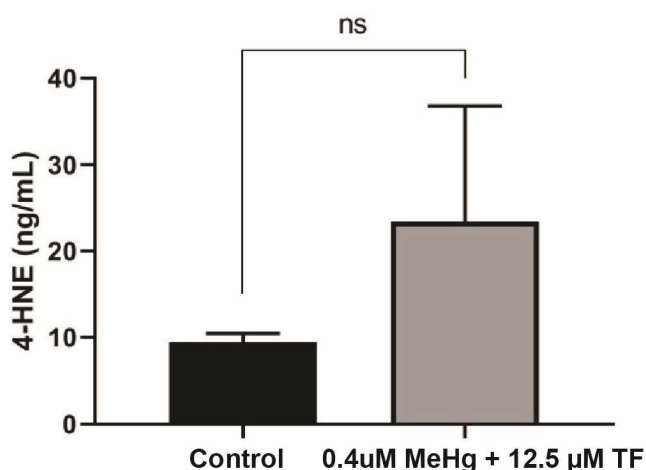


Figure 3.4e: 4-HNE secretion from control cells (population 1) and MeHg + 12.5 μM TF-3 exposed cells (population 5) from day 18 - day 28; p-value was 0.0892

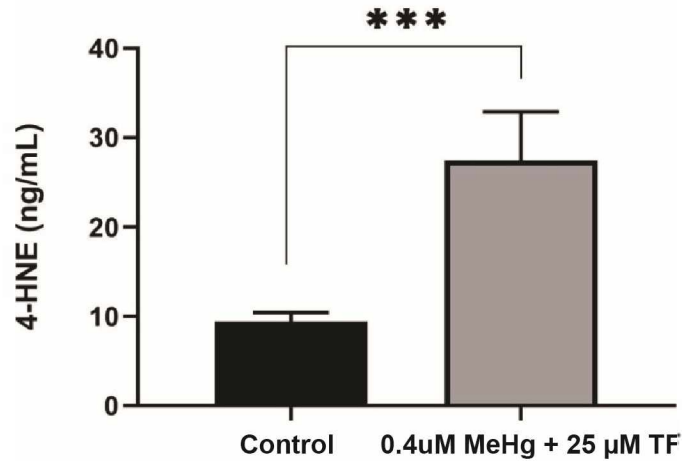


Figure 3.4f: 4-HNE secretion from control cells (population 1) and MeHg + 25 μM TF-3 exposed cells (population 6) from day 18 - day 28; p-value was less than 0.0001.

Populations 7 and 8 secreted lowest 4-HNE levels. This suggests greater concentrations of TF-3 are not appropriate for either adipokines or 4-HNE productions. The average value of 4-HNE in population 7 was 2.3 ± 0.5 ng/mL, however data obtained is significant having a p value < 0.0001 using Student's T-test (Figure 3.4g). 4-HNE levels from population 8 was reported as 2.1 ± 0.6 ng/mL, when compared against population 1 using Student's T test, it was found that data presented is significantly different having a p-value < 0.0001 (Figure 3.4h).

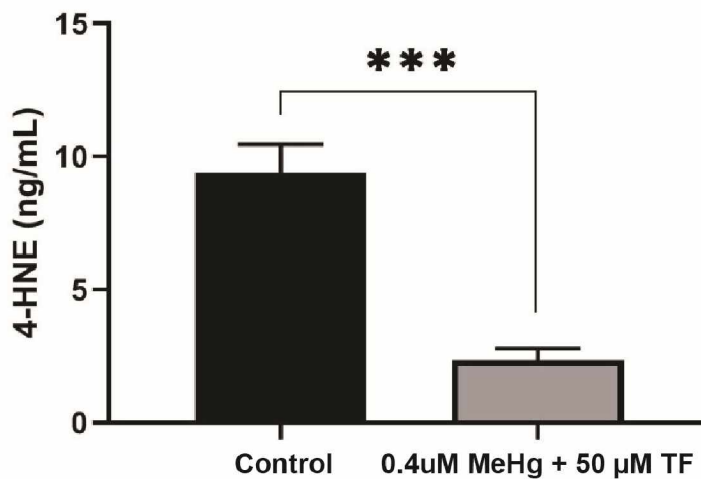


Figure 3.4g: 4-HNE secretion from control cells (population 1) and MeHg + 50 μM TF-3 exposed cells (population 7) from day 18 - day 28; p-value was less than 0.0001.

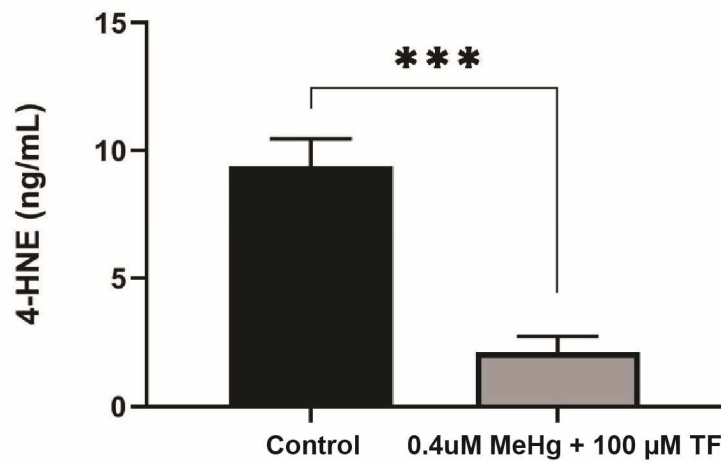


Figure 3.4h: 4-HNE secretion from control cells (population 1) and MeHg + 100 μ M TF-3 exposed cells (population 8) from day 18 - day 28; p-value was less than 0.0001.

Overall, MeHg did increase 4-HNE levels and 3.14 and 6.25 μ M TF-3 were able to restore the increased levels closer to population 1(control) 4-HNE level.

Chapter 4: Discussion

This study aimed to determine the effects of MeHg and TF-3 on the morphology, two adipokines and 4-HNE secretions from 3T3-L1 adipocytes. To understand how the secretion patterns of adiponectin, resistin and 4-HNE are affected, 3T3-L1 cells were cultured to mature adipocytes and treated with 0.4 μ M MeHg. Different concentrations of TF-3 were added to 0.4 μ M MeHg treated 3T3-L1 adipocytes to determine if oxidative stress markers could be observed and if any TF-3 concentration negated the effects of MeHg.

Alaskan Natives, due to subsistence lifestyle, are constantly exposed to mercury, particularly MeHg, through fish consumption (Hamade, 2014). Barnes et al in 2003 and 2005 showed that mercury exposure (inorganic) interferes with the process of adipogenesis, increased glucose uptake in 3T3-L1 adipocytes (Barnes et al., 2003, 2005). In 2017, Vertigan et al. reported the effect of MeHg on VEGF, a cytokine, in 3T3-L1 cells secretions (Vertigan et al., 2017). These prior mercury studies provided basis for further research on 3T3-L1 cells. To the best of our knowledge, no study exist which examines the effect of MeHg and the anti-inflammatory TF-3, on the secretions of two adipokines (adiponectin and resistin) and 4-HNE levels in 3T3-L1 adipocytes.

MeHg initiates chemical reactions that result in ROS production, which eventually increases lipid peroxidation and the generation of 4-HNE, a stable product of lipid peroxidation (Hong et al., 2012; Borza et al., 2013). The increase in MeHg induced ROS levels is hypothesized to change adipokines secretion patterns in 3T3-L1 cells. Overall, increased 4-HNE levels as a marker in oxidative stress among the cells was observed and resulted in different secretion patterns of adiponectin and resistin.

Increasing rates of type 2 diabetes and hypertension are often associated with obesity with mild and/or chronic inflammation conditions. I addressed the question of whether MeHg promotes the pro-inflammatory signs leading to a chronic inflammatory disease state. An

inflammatory condition is reported in metabolic syndrome and cardiovascular diseases. Since adipokines commonly play roles in these diseases and are considered as biomarker for inflammation, oxidative stress and metabolic syndrome, the effect of an anti-inflammatory natural product to counteract 4-HNE and return the adipokines to control levels was tested.

4.1 Morphology changes in 3T3-L1 adipocytes

3T3-L1 preadipocytes were grown into mature adipocytes to determine the effects of MeHg and TF-3 on the morphology of the treated cells. Results suggest that 0.4 μM (100 ng/mL) MeHg did alter the normal spherical morphology of the healthy cells resulting in fewer numbers and distortion of adipocytes. Overall from day 18 to day 28, MeHg induced apoptosis was evident in population 2 which suggests that MeHg stressed the cells by altering the redox conditions. Most of the fat globules had smaller sized droplets and cells were highly agglomerated (Figure 3.1h; population 2). Lipid staining on day 28 of the culture study showed less stained lipid droplets in population 2 (0.4 μM MeHg treatment) when compared to control cells.

Treatment with a range of different concentrations of TF-3 was carried out on MeHg exposed cells. During initial days of treatment (days 18 - 24), 3.14 μM , 6.25 μM , 12.5 μM and 25 μM were able to counteract MeHg induced changes as seen in population 2 (Figure 3.1h; populations 2-6). Cells at these concentrations of TF-3 populations looked comparatively healthier with less clumping and bigger fat globules than cells in population 2, even though murkiness could be seen around these populations. During the last four days (days 24 - 28) of study, 6.25 μM TF-3 concentration had the highest number of stained cells when compared to control. Other tea concentrations such as 3.14 μM , 12.5 μM , 25 μM , 50 μM and 100 μM had larger and less clumped lipid droplets but were less in number. The TF-3 concentrations showed a dose dependent response in maintaining normal cell morphology while being constantly exposed to MeHg.

The data suggests that TF-3 has neutralized some of the increased ROS and reduced the increased oxidative stress. TF-3 reduced the effect of MeHg and helped the MeHg exposed cells to have a normal morphology similar to control group (Figure 3.1h; populations 1 - 8). Further analyses of the effect of TF-3 on MeHg exposed cells will give a clearer picture.

Morphology does not necessarily tell much about the secretion levels of adipokines. It does however suggest an underlying stressful cellular environment in these cell populations.

4.2 Adiponectin secretion from MeHg exposed 3T3-L1 adipocytes and counter effects of TF-3 on MeHg exposed cells.

Adiponectin is one of the biomarkers reported to determine normal metabolic status of the human body (Zhang et al., 2015a). It is mostly secreted from adipose tissue. Adiponectin levels are associated with metabolic syndrome related diseases, cardiovascular diseases and autoimmune diseases (Meier, 2004; Apprahamian & Sam, 2011). In this study, adiponectin levels were determined for ten days in mature adipocytes. Cells were treated with 0.4 μ M MeHg and different concentrations of TF-3 (3.14, 6.25, 12.5, 25, 50 and 100 μ M). MeHg exposure increased levels of adiponectin when compared to control cells (Figure 3.2b). This increase suggested an increase in inflammatory activities induced in a cell system, since adiponectin can act as an anti-inflammatory and antioxidative (Diez & Iglesias., 2003; Lago et al., 2007). Earlier reports suggest that adiponectin increased in chronic inflammatory related diseases; however, the reason for this increase remains unknown (Apprahamian & Sam, 2011). Data suggest that higher adiponectin levels are associated with increase in inflammatory and oxidative conditions in exposed cells.

In the MeHg treated cells, some TF-3 concentrations showed their antioxidative properties by reducing the increased concentration of adiponectin. 3.14 μ M TF-3 did not counteract the effects of 0.4 μ M MeHg (Figure 3.2c), however 6.25 μ M and 12.5 μ M TF-3 were able to slightly reduce the increased adiponectin levels (Figures 3.2 d and e). The best

response was obtained from 25 μ M TF-3 since it restored the increased adiponectin levels close to that of control cells (Figure 3.2f).

50 and 100 μ M TF-3 decreased adiponectin levels even lower than that of control cells suggesting greater concentrations of TF-3 are not an appropriate dosage in combating the MeHg exposure (Figures 3.2g and h). High concentration of TF-3 might interfere with the natural oxidant (ROS) - anti inflammatory compound balance.

4.3 Resistin secretion from MeHg exposed 3T3-L1 adipocytes and counter effects of TF-3 on MeHg exposed cells.

Compared to adiponectin, resistin is a relatively newly-studied adipokine. It is still under study to explore its role in cellular processes. It may be a link that connects obesity and type 2 diabetes (Berger, 2001; Steppan et al., 2001). Resistin is an anti-inflammatory marker for cardiovascular diseases (Reilly et al., 2005; Zhang et al., 2015a). Higher levels of resistin are found in a condition of insulin resistance (Ding et al., 2012). In this study, resistin levels were measured in cell culture media collected from mature adipocytes in order to determine effects of MeHg and different concentrations of TF-3. Our data showed that MeHg increased the mean resistin levels in exposed 3T3-L1 cells (Figure 3.3b). Resistin levels were drastically decreased during the last four days (days 24 – 28), but overall there was an increase in resistin concentration. This suggests that cells were under oxidative stress. Since resistin is an anti-inflammatory factor, the higher resistin levels were seen in MeHg treated adipocytes population. Why resistin levels decreased during last four days but adiponectin levels increased gradually might indicate an autocrine feedback mechanism is present.

From the data, resistin levels are very sensitive to TF-3 treatment because even 3.14 μ M TF-3 was effective in restoring mean resistin levels close to control cells' resistin level (Figure 3.3c). Higher TF-3 concentrations decrease resistin levels gradually. Further research will provide more reasoning behind this effectiveness. TF-3 at 25, 50 and 100 μ M reduced resistin

levels drastically lower than control cells (Figures 3.3 f, g and h). The best TF-3 concentration that restored the increased resistin level closest to the control group was 3.14 μ M. This concentration neutralized the increased ROS levels in MeHg treated cells thereby reducing oxidative stress.

4.4 4-HNE secretion from MeHg exposed 3T3-L1 adipocytes and counter effects of TF-3 on MeHg exposed cells.

4-HNE is a product of lipid peroxidation and increases in cells under oxidative stress (Borza et al., 2013; Zhong & Yin, 2015). Increased levels of 4-HNE have been reported in aging, diabetes, obesity and neurodegenerative diseases (Dasuri et al., 2012). Our data indicate that exposure to MeHg significantly increased 4-HNE level in 3T3-L1 mature adipocytes (Figure 3.4b).

In MeHg exposed populations treated with 3.14 and 6.25 μ M TF-3 levels returned to control levels (Figures 3.4c and d). 3.14 μ M was more effective in restoring 4-HNE levels closer to that of control cells while 50 and 100 μ M TF-3 resulted in lower levels of 4-HNE than control populations, suggesting that higher concentrations of TF-3 increased stress which may have lead to cellular apoptosis (Figures 3.4g and h). In populations treated with 12.5 and 25 μ M TF-3 since 4-HNE levels were greatly increased suggesting an extensive imbalance between oxidants and anti oxidants levels in cells (Figures 3.4e and f).

4.5 Future directions

In this study, a cell system model to determine the effects of MeHg and TF-3 on the adipocytes on a biochemical scale was developed. This model can further be used to determine the effects of other heavy metals on adipokines secretion levels. Determination of particular reactive oxygen and nitrogen species will be more beneficial in order to know exact difference before and after exposure. This would support our central hypothesis that MeHg increases

basal ROS levels which further lipid peroxidation and affects various interconnected cellular processes.

The mechanism of activating the resistin increase at the genetic level by MeHg or any other heavy metal should be explored. Future studies should also include working on the unknown mechanism of MeHg toxicity in different cell types. Different adipokines other than adiponectin and resistin can be studied to investigate MeHg induced changes. Different TF-3 concentrations can be used to have a clearer understanding of the anti oxidative effects of polyphenolic compounds. Determining effects of different polyphenols extracted from natural sources in withstanding detrimental effects of heavy metals on cell types will provide a healthy research ground in the field of toxicology.

References

- Aprahamian, T. R., & Sam, F. (2011). Adiponectin in Cardiovascular Inflammation and Obesity. *International Journal of Inflammation*, 2011, 1-8.
- Ballew, C., Ross, A., Wells, R. S., & Hiratsuka, V. (2004). *Final report on the Alaska Traditional Diet Survey*. (Rep.). Anchorage, AK: Alaska Native Health Board.
- Barnes, D. M., Hanlon, P. R., & Kircher, E. A. (2003). Effects of Inorganic HgCl₂ on Adipogenesis. *Toxicological Sciences*, 75 (2), 368-377.
- Barnes, D. M., & Kircher, E. A. (2005). Effects of mercuric chloride on glucose transport in 3T3-L1 adipocytes. *Toxicology in Vitro*, 19 (2), 207-214.
- Bays, H. E., González-Campoy, J. M., Bray, G. A., Kitabchi, A. E., Bergman, D. A., Schorr, A. B., Rodbard, H. W., & Henry, R. R. (2008). Pathogenic potential of adipose tissue and metabolic consequences of adipocyte hypertrophy and increased visceral adiposity. *Expert Review of Cardiovascular Therapy*, 6 (3), 343-368.
- Beltowski, J. (2003). Adiponectin and resistin-new hormones of white adipose tissue. *Med Sci Monit*, 9 (2), RA55-61.
- Berger, A. (2001). Resistin: a New Hormone That Links Obesity with Type 2 Diabetes. *The British Medical Journal*, 322 (7280), 193.
- Borza, C., Șerban, C., Dehelean, C., Muntean, D., Simu, G., Săvoiu, G., Butur, M., Andoni, M., & Drăgan, S. (2013). *Oxidative Stress and Lipid Peroxidation - A Lipid Metabolism Dysfunction*. INTECH Open Access Publisher.
- Brody, R., Peleg, E., Grossman, E., & Sharabi, Y. (2009). Production and Secretion of Adiponectin from 3T3-L1 Adipocytes: Comparison of Antihypertensive Drugs. *American Journal of Hypertension*, 22 (10), 1126-1129.
- Castro, J. P., Grune, T., & Speckmann, B. (2016). The two faces of reactive oxygen species (ROS) in adipocyte function and dysfunction. *Biological Chemistry*, 397 (8), 709-24.
- Chen, Y. W., Huang, C. F., Tsai, K. S., Yang, R. S., Yen, C. C., Yang, C. Y., Lin-Shiau, S. Y., & Liu, S. H. (2006). Methylmercury Induces Pancreatic β -Cell Apoptosis and Dysfunction. *Chemical Research in Toxicology*, 19 (8), 1080-1085.
- Coelho, M., Oliveira, T., & Fernandes, R. (2013). State of the art paper Biochemistry of adipose tissue: An endocrine organ. *Archives of Medical Science*, 2, 191-200.
- Dasuri, K., Ebenezer, P., Fernandez-Kim, S. O., Zhang, L., Gao, Z., Bruce-Keller, A. J., Freeman, L.R., & Keller, J. N. (2012). Role of physiological levels of 4-hydroxynonenal on adipocyte biology: Implications for obesity and metabolic syndrome. *Free Radical Research*, 47(1), 8-19.

Department of Health and Human Services. (2012, June). Diabetes in American Indians and Alaska Natives, Facts At-a-Glance. Retrieved April 17, 2019, from https://www.ihs.gov/MedicalPrograms/Diabetes/HomeDocs/Resources/FactSheets/Fact_sheet_AIAN_508c.pdf

Diez, J., & Iglesias, P. (2003). The role of the novel adipocyte-derived hormone adiponectin in human disease. *European Journal of Endocrinology*, 148, 293-300.

Ding, M., Rzucidlo, E. M., Davey, J. C., Xie, Y., Liu, R., Jin, Y., Stavola, N., & Martin, K. A. (2012). Adiponectin in the Heart and Vascular System. *Adiponectin Vitamins & Hormones*, 90, 289-319.

Dunmore, S. J., & Brown, J. E. (2012). The role of adipokines in β -cell failure of type 2 diabetes. *Journal of Endocrinology*, 216 (1), T37-45.

Erickson, P. R., & Lin, V. S. (2015). Research highlights: Elucidation of biogeochemical factors influencing methylmercury production. *Environmental Science: Processes & Impacts*, 17 (10), 1708-1711.

Fasshauer, M., Kralisch, S., Klier, M., Lossner, U., Bluher, M., Klein, J., & Paschke, R. (2003). Adiponectin gene expression and secretion is inhibited by interleukin-6 in 3T3-L1 adipocytes. *Biochemical and Biophysical Research Communications*, 301 (4), 1045-1050.

Futatsuka, M., Kitano, T., & Wakamiya, J. (1996). An Epidemiological Study on Diabetes Mellitus in the Population Living in a Methyl Mercury Polluted Area. *Journal of Epidemiology*, 6 (4), 204-208.

Gao, Y., Rankin, G. O., Tu, Y., & Chen, Y. C. (2015). Theaflavin-3, 3'-digallate decreases human ovarian carcinoma OVCAR-3 cell-induced angiogenesis via Akt and Notch-1 pathways, not via MAPK pathways. *International Journal of Oncology*, 48 (1), 281-292.

Gregoire, F. M., Smas, C. M., & Sul, H. S. (1998). Understanding Adipocyte Differentiation. *Physiological Reviews*, 78 (3), 783-809.

Guilherme, A., Virbasius, J. V., Puri, V., & Czech, M. P. (2008). Adipocyte dysfunctions linking obesity to insulin resistance and type 2 diabetes. *Nature Reviews Molecular Cell Biology*, 9 (5), 367-377.

Hamade, A. K. (2014). *Fish Consumption Advice for Alaskan: Risk Management Strategy To Optimize the Public's Health* (pp. 1-78).

He, K., Xun, P., Liu, K., Morris, S., Reis, J., & Guallar, E. (2013). Mercury Exposure in Young Adulthood and Incidence of Diabetes Later in Life: The CARDIA Trace Element Study. *Diabetes Care*, 36 (6), 1584-1589.

Heilbronn, L., & Campbell, L. (2008). Adipose Tissue Macrophages, Low Grade Inflammation and Insulin Resistance in Human Obesity. *Current Pharmaceutical Design*, 14 (12), 1225-1230.

Hong, Y., Kim, Y., & Lee, K. (2012). Methylmercury Exposure and Health Effects. *Journal of Preventive Medicine & Public Health*, 45 (6), 353-363.

- Jonas, M. I., Kurylowicz, A., Bartoszewicz, Z., Lisik, W., Jonas, M., Domienik-Karłowicz, J., & Puzianowska-Kuznicka, M. (2017). Adiponectin/resistin interplay in serum and in adipose tissue of obese and normal-weight individuals. *Diabetology & Metabolic Syndrome*, 9, 1-9.
- Kahn, S. E., Hull, R. L., & Utzschneider, K. M. (2006). Mechanisms linking obesity to insulin resistance and type 2 diabetes. *Nature*, 444 (7121), 840-846.
- Kanda, H., Shinkai, Y., & Kumagai, Y. (2014). S-Mercuration of cellular proteins by methylmercury and its toxicological implications. *The Journal of Toxicological Sciences*, 39 (5), 687-700.
- Kerper, L. E., Ballatori, N., & Clarkson, T. W. (1992). Methylmercury transport across the blood-brain barrier by an amino acid carrier. *American Journal of Physiology-Regulatory, Integrative and Comparative Physiology*, 262 (5).
- Koerner, A., Kratzsch, J., & Kiess, W. (2005). Adipocytokines: Leptin—the classical, resistin—the controversial, adiponectin—the promising, and more to come. *Best Practice & Research Clinical Endocrinology & Metabolism*, 19 (4), 525-546.
- Kohlgruber, A., & Lynch, L. (2015). Adipose Tissue Inflammation in the Pathogenesis of Type 2 Diabetes. *Current Diabetes Reports*, 15 (11).
- Krabbenhoft, D. P., & Sunderland, E. M. (2013). Global Change and Mercury. *Science*, 341 (6153), 1457-1458.
- Kumagai, Y., Kanda, H., Shinkai, Y., & Toyama, T. (2013). The Role of the Keap1/Nrf2 Pathway in the Cellular Response to Methylmercury. *Oxidative Medicine and Cellular Longevity*, 2013, 1-8.
- Lago, F., Dieguez, C., Gomezreino, J., & Gualillo, O. (2007). The emerging role of adipokines as mediators of inflammation and immune responses. *Cytokine & Growth Factor Reviews*, 18(3-4), 313-325.
- Lau, C., & Muniandy, S. (2011). Novel adiponectin-resistin (AR) and insulin resistance (IRAR) indexes are useful integrated diagnostic biomarkers for insulin resistance, type 2 diabetes and metabolic syndrome: A case control study. *Cardiovascular Diabetology*, 10 (1), 8.
- Lemire, M., Kwan, M., Laouan-Sidi, A., Muckle, G., Pirkle, C., Ayotte, P., & Dewailly, E. (2015). Local country food sources of methylmercury, selenium and omega-3 fatty acids in Nunavik, Northern Quebec. *Science of The Total Environment*, 509, 248-259.
- Magueresse-Battistoni, B. L., Vidal, H., & Naville, D. (2018). Environmental Pollutants and Metabolic Disorders: The Multi-Exposure Scenario of Life. *Frontiers in Endocrinology*, 9.
- Mahaffey, K. R. (1999). Methylmercury: A new look at the risks. *Public Health Reports*, 114 (5), 397-413.

- Makhoul, Z., Kristal, A. R., Gulati, R., Luick, B., Bersamin, A., Boyer, B., & Mohatt, G. V. (2010). Associations of very high intakes of eicosapentaenoic and docosahexaenoic acids with biomarkers of chronic disease risk among Yup'ik Eskimos. *The American Journal of Clinical Nutrition*, 91 (3), 777-785.
- Mattson, M. P. (2009). Roles of the lipid peroxidation product 4-hydroxynonenal in obesity, the metabolic syndrome, and associated vascular and neurodegenerative disorders. *Experimental Gerontology*, 44 (10), 625-633.
- Meier, U. (2004). Endocrine Regulation of Energy Metabolism: Review of Pathobiochemical and Clinical Chemical Aspects of Leptin, Ghrelin, Adiponectin, and Resistin. *Clinical Chemistry*, 50 (9), 1511-1525.
- Meo, S. D., Reed, T. T., Venditti, P., & Victor, V. M. (2016). Harmful and Beneficial Role of ROS. *Oxidative Medicine and Cellular Longevity*, 2016, 1-3.
- Miao, M., Jiang, H., Jiang, B., Li, Y., Cui, S. W., & Jin, Z. (2013). Elucidation of structural difference in theaflavins for modulation of starch digestion. *Journal of Functional Foods*, 5 (4), 2024-2029.
- Murdolo, G., & Smith, U. (2006). The dysregulated adipose tissue: A connecting link between insulin resistance, type 2 diabetes mellitus and atherosclerosis. *Nutrition, Metabolism and Cardiovascular Diseases*, 16, S35-S38.
- Nobmann, E. D., Byers, T., Lanier, A. P., Hankin, J. H., & Jackson, M. Y. (1992). The diet of Alaska Native adults: 1987–1988. *The American Journal of Clinical Nutrition*, 55 (5), 1024-1032.
- Parnell, S., Streur, W. J., Shelton, K., & Allely, K. (2014). *Alaska Obesity Facts* (pp. 6-51, Rep.). Anchorage, Alaska: Alaska Department of Health and Social Services.
- Reilly, M. P., Lehrke, M., Wolfe, M. L., Rohatgi, A., Lazar, M. A., & Rader, D. J. (2005). Resistin Is an Inflammatory Marker of Atherosclerosis in Humans. *Circulation*, 111(7), 932-939.
- Rizzatti, V., Boschi, F., Pedrotti, M., Zoico, E., Sbarbati, A., & Zamboni, M. (2013). Lipid droplets characterization in adipocyte differentiated 3T3-L1 cells: Size and optical density distribution. *European Journal of Histochemistry*, 57 (3), 24.
- Scherer, P. E. (2006). Adipose Tissue: From Lipid Storage Compartment to Endocrine Organ. *Diabetes*, 55 (6), 1537-1545.
- Steppan, C. M., Bailey, S. T., Bhat, S., Brown, E. J., Banerjee, R. R., Wright, C. M., Patel, H.R., Ahima, R.S., & Lazar, M. A. (2001). The hormone resistin links obesity to diabetes. *Nature*, 409 (6818), 307-312.
- Szendrodi, J. (2004). The adipose tissue as an endocrine organ. *Acta Med Austriaca*, 1: 98-111.
- Timar, R., Timar, B., Degeratu, D., Serafinceanu, C., & Oancea, C. (2014). Metabolic syndrome, adiponectin and proinflammatory status in patients with type 1 diabetes mellitus. *Journal of International Medical Research*, 42(5), 1131-1138.

- United States Environmental Protection Agency. (2015, October 19). Mercury Study Report to Congress. Retrieved from <https://www.epa.gov/mercury/mercury-study-report-congress>
- Vertigan, T., Dunlap, K., Reynolds, A., & Duffy, L. (2017). Effects of Methylmercury exposure in 3T3-L1 Adipocytes. *AIMS Environmental Science*, 4 (1), 94-111.
- Weiss, B. (2007). Why Methylmercury Remains a Conundrum 50 Years after Minamata. *Toxicological Sciences*, 97 (2), 223-225.
- Weyer, C. (2001). Hypoadiponectinemia in Obesity and Type 2 Diabetes: Close Association with Insulin Resistance and Hyperinsulinemia. *Journal of Clinical Endocrinology & Metabolism*, 86 (5), 1930-1935.
- World Health Organization. (1990). *Methylmercury: Published under the joint sponsorship of the United Nations Environment Programm*. Geneva: World Health Organization.
- Wu, W., Jiang, S., Zhao, Q., Zhang, K., Wei, X., Zhou, T., Liu, D., Zhou, H., Zeng, Q., Cheng, L., Miao, X., & Lu, Q. (2018). Environmental exposure to metals and the risk of hypertension: A cross-sectional study in China. *Environmental Pollution*, 233, 670-678.
- Wu, X., Beecher, G. R., Holden, J. M., Haytowitz, D. B., Gebhardt, S. E., & Prior, R. L. (2004). Lipophilic and Hydrophilic Antioxidant Capacities of Common Foods in the United States. *Journal of Agricultural and Food Chemistry*, 52 (12), 4026-4037.
- Wu, Y., Jin, F., Wang, Y., Li, F., Wang, L., Wang, Q., Ren, Z., & Wang, Y. (2017). In vitro and in vivo anti-inflammatory effects of theaflavin-3,3'-digallate on lipopolysaccharide-induced inflammation. *European Journal of Pharmacology*, 794, 52-60.
- Zahorska-Markiewicz, B. (2006). Metabolic effects associated with adipose tissue distribution. *Adv Med Sci*, 51:111-114.
- Zhang, J., Kho, P., OV, K., & Chenghe, S. (2015a). Adiponectin, Resistin and Leptin: Possible Markers of Metabolic Syndrome. *Endocrinology & Metabolic Syndrome*, 04 (04).
- Zhang, J., Zhang, Z., Ding, Y., Xu, P., Wang, T., Xu, W., Lu, H., Li, J., Wang, Y., & Xie, J. (2015b). Adipose Tissues Characteristics of Normal, Obesity, and Type 2 Diabetes in Uyghurs Population. *Journal of Diabetes Research*, 2015, 1-6.
- Zhong, H., & Yin, H. (2015). Role of lipid peroxidation derived 4-hydroxynonenal (4-HNE) in cancer: Focusing on mitochondria. *Redox Biology*, 4, 193-199.
- Zou, C., & Shao, J. (2008). Role of adipocytokines in obesity-associated insulin resistance. *The Journal of Nutritional Biochemistry*, 19 (5), 277-286.